Accepted for publication in *Transportation Science*, June 2020

The robust vehicle routing problem with time window assignments

Maaike Hoogeboom
Department of Supply Chain Analytics, Vrije Universiteit Amsterdam, 1081 HV Amsterdam, The Netherlands, m.hoogeboom@vu.nl,

Yossiri Adulyasak
HEC Montréal and GERAD, Montréal, H3T 2A7, Canada, yossiri.adulyasak@hec.ca,

Wout Dullaert
Department of Supply Chain Analytics, Vrije Universiteit Amsterdam, 1081 HV Amsterdam, The Netherlands, wout.dullaert@vu.nl,

Patrick Jaillet
Department of Electrical Engineering and Computer Science, Operations Research Center, Massachusetts Institute of Technology, Cambridge, MA 02139, jaillet@mit.edu,

In practice, there are several applications in which logistics service providers determine the service time window at the customers, e.g., in parcel delivery, retail and repair services. These companies face uncertain travel times and service times that have to be taken into account when determining the time windows and routes prior to departure. The objective of the proposed robust vehicle routing problem with time window assignments (RVRP-TWA) is to simultaneously determine routes and time window assignments such that the expected travel time and the risk of violating the time windows are minimized. We assume that the travel time probability distributions are not completely known but that some statistics, such as the mean, minimum, and maximum, can be estimated. We extend the robust framework based on the requirements violation (RV) index, which was originally developed for the case where the specific requirements (time windows) are given as inputs, to the case where they are also part of the decisions. The subproblem of finding the optimal time window assignment for the customers in a given route is shown to be convex and the subgradients can be derived. The RVRP-TWA is solved by iteratively generating subgradient cuts from the subproblem that are added in a branch-and-cut fashion. Experiments address the performance of the proposed solution approach and examine the trade-off between expected travel time and risk of violating the time windows.

Key words: vehicle routing, time window assignment, robust optimization, uncertain travel times

1. Introduction

In the vehicle routing problem with time windows, service time windows are typically an input. In practice, however, there are many cases in which time windows are imposed by the service provider or are based on a mutual agreement or service-level agreement between the service provider and the customer. This is the case in attended home deliveries, for example furniture delivery (Jabali et al. 2015), online grocery (Campbell and Savelsbergh 2006), internet installation (Ulmer and Thomas 2019), and repair and maintenance services (Vareias, Repoussis, and Tarantilis 2017). When determining service time windows, there are often conflicting interests between customers and the service provider. On the one hand, customers typically prefer narrow time windows to limit the waiting time and to better plan their daily activities. The economic loss resulting from waiting for service at home was estimated at $38 billion in the USA in 2011 (Ellis 2011, Ulmer and Thomas 2019). On the other hand, service providers prefer wide time windows to have more routing flexibility and to lower the risk of violating the time window due to travel and service time uncertainties.

When planning an attended home delivery or service, customers can, in most cases, indicate an exogenous time window consisting of several hours during which they are available for service (Agatz et al. 2011, Klein et al. 2017). To improve the service and satisfaction of customers, service providers can then assign a smaller endogenous time window to each customer. The service providers, however, are faced with uncertain travel and service times that have to be taken into account when determining these endogenous time windows. This chapter considers the case in which a set of routes and endogenous time windows have to be generated before the travel times are known. The goal is to generate a robust routing plan and assign time windows to customers such that the risk of violating the time windows is minimized and the expected total travel time is below a certain threshold value.

The vehicle routing problem with time window assignments (VRP-TWA) and uncertain demand was introduced by Spliet and Gabor (2014). In this problem, time windows have to be assigned to customers before demand is known. When the demand is revealed, a vehicle routing schedule has to be generated that satisfies the assigned time windows. Spliet and Gabor (2014) assume that there is a set of demand scenarios that can occur and that a time windows assignment that minimizes the average routing cost over these scenarios has to be found. Jabali et al. (2015) introduce a similar problem in which the demand is known but the travel times are uncertain. They assume that a disruption on an arc can occur with a certain probability and that the duration of this disruption is a discrete random variable with a known probability function. To reduce the number of scenarios, they assume that a disruption occurs on exactly one arc in a solution. The goal is to find an a priori routing plan and time window assignment that minimizes travel cost and time window

violations. Vareias, Repoussis, and Tarantilis (2017) extend the work of Jabali et al. (2015) by allowing multiple arcs to be disrupted and by letting the duration of a disruption be a continuous random variable. They also propose a second model in which the travel time of each arc is a discrete random variable. Both Jabali et al. (2015) and Vareias, Repoussis, and Tarantilis (2017) solve a stochastic variant of the VRP-TWA in which the probability distributions are completely known and in both papers a heuristic solution method is proposed. To handle cases where the probability distributions are hard to estimate, a robust optimization model can be used.

In this chapter, the robust time window assignment vehicle routing problem (RVRP-TWA) is formulated in which the travel time probability functions are uncertain and only some descriptive statistics such as mean, minimum, and maximum travel times are available. To measure the risk of violating the assigned time windows, the time window violation index proposed in Jaillet, Qi, and Sim (2016) is used. This measure incorporates the distributional statistics and is therefore less conservative than classical robust approaches where this information is ignored. Furthermore, both the frequency and magnitude of a violation are taken into account in this measure. The objective of the RVRP-TWA is to find routes and time window assignments that minimize the time window violation index. A solution method is proposed to solve the subproblem of finding the optimal time window assignment for each customer in a given route. By using a subgradient method implemented in a branch-and-cut framework, the RVRP-TWA is solved to optimality. The stochastic VRP-TWA (SVRP-TWA) is also discussed and used to illustrate the potential of the robust model. In the SVRP-TWA, the probability distributions of the travel times are assumed to be known and the average time window violation is minimized while the expected total travel time should be lower than a certain value. The SVRP-TWA is solved exactly using a branch-and-cut approach.

The main contributions of this research are as follows. (1) We are the first to propose a robust formulation for the VRP-TWA based on the risk measure proposed by Jaillet, Qi, and Sim (2016). (2) An efficient algorithm to optimize the time window assignments for a given set of routes is proposed. We show that this subproblem of finding the optimal time window assignment for a given route is convex and the subgradient can be derived which allows for an efficient solution method. (3) A decomposition method is proposed to exactly solve the RVRP-TWA using the subgradient method in a branch-and-cut framework. (4) An exact solution method is proposed to solve the stochastic VRP-TWA. (5) Extensive computational experiments are performed to provide insights of working with limited data and to create a Pareto frontier of risk and expected total travel time.

The remainder of this chapter is organized as follows. In Section 2, the literature on robust vehicle routing and VRP-TWA is reviewed. In Section 3, the RVRP-TWA and the feasible routing set are formally described. In Section 4, the robust solution framework is presented and the subproblem

of finding the optimal time window assignment problem for a given route is solved. The branch-and-cut framework is presented in Section 5. The stochastic version of the VRP-TWA is proposed in Section 6. In Section 7, the computational results are discussed and conclusions are presented in the final section.

2. Literature review

The vehicle routing problem (VRP) and many of its deterministic variants have been extensively studied, for literature reviews see e.g., Golden, Raghavan, and Wasil (2008), Toth and Vigo (2014). In practice, however, many parameters such as customer demand, customer location and travel times are uncertain. Since larger amounts of data are becoming available, there has been an increase in the number of studies addressing the uncertain variants of the vehicle routing problem (Gendreau, Jabali, and Rei 2016). Generally speaking, there are two ways to deal with uncertainty: a stochastic approach in which the distribution of the uncertain parameter is known and a robust approach in which the probability distribution is hard to justify or estimate. The VRP with stochastic travel times was introduced by Laporte, Louveaux, and Mercure (1992) and extended by many others (Gendreau, Jabali, and Rei 2016). The extension of including time windows is considered in e.g., Russell and Urban (2008), Taş et al. (2013, 2014), Ehmke, Campbell, and Urban (2015), Adulyasak and Jaillet (2016). In the robust VRP, uncertain parameters are characterized by uncertainty sets without information on the probability function, see e.g. Ordóñez (2010) for an overview. Recent studies present solution frameworks that incorporate some statistical information in the robust approach. For example, Lee, Lee, and Park (2012) and Agra et al. (2013) solve the VRPTW in which travel time uncertainty is defined using the budget of uncertainty as introduced by Bertsimas and Sim (2004). Jaillet, Qi, and Sim (2016) propose a method to solve the TSP with time windows in which the probability distributions of the travel times are unknown but some descriptive statistics, as the mean, minimum, and maximum values, are known. They define a mathematical framework to solve this problem in an efficient and exact way. They propose a new measure to quantify the risk of violating a time window taking into account both the frequency and the magnitude of the violations. The routing problem with the objective of minimizing the risk measure is solved using the Benders decomposition technique. The authors showed that their robust solution approach is superior to existing models. Adulyasak and Jaillet (2016) extend this model to multiple vehicles and propose a stochastic model in which the probability distributions of the travel times are assumed to be known. Adulyasak and Jaillet (2016) were able to significantly reduce the computational time, compared to Jaillet, Qi, and Sim (2016), by using a branch-and-cut solution approach.

Zhang et al. (2019) propose a modification of the risk measure of Jaillet, Qi, and Sim (2016), to handle the TSP with hard time window as opposed to soft time window. They assume that a vehicle

can wait at no cost at the location of the customer if it arrives before the time window but arriving after the time window should be avoided. Their proposed risk measure is less tight in measuring the probability of violation, but allows for a more tractable formulation for the VRP with hard time windows. Zhang et al. (2018) extend the measure of Zhang et al. (2019) by incorporating a parameter to customize the service level in terms of probabilistic guarantee of on-time delivery. They propose a data-driven framework using the Wasserstein ambiguity set which is derived from empirical travel time data. In this chapter, we are dealing with soft time windows, where waiting at a customer before the start of the time window is impossible or costly.

In all the papers discussed above, the time windows are input so they do not consider the time window assignment problem. Therefore, the frameworks of Jaillet, Qi, and Sim (2016) and Adulyasak and Jaillet (2016) cannot be directly applied to solve the proposed RVRP-TWA since the time windows are now decision variables instead of inputs. We will show that the new robust formulation is convex and that the subgradient can be derived. To measure the risk of violating the assigned time windows, the time window violation index proposed by Jaillet, Qi, and Sim (2016) will be used. A branch-and-cut approach, adapted from the original approach proposed in Adulyasak and Jaillet (2016), is developed to solve the RVRP-TWA.

The problem of assigning time windows to customers has recently been introduced by Spliet and Gabor (2014) to solve a retail distribution problem. They propose the VRP-TWA with uncertain demand in which the deliveries to a store should always be made in the same fixed time window while demand fluctuates per delivery. They assume that there is a set of demand scenarios that can occur and that the best time windows assignment over these scenarios has to be found. In this VRP-TWA, the time windows have to be assigned before the demand is known but the routes are made after the demand is revealed. As such, a different route per demand scenario has to be determined in the optimization process. The problem is solved using a branch-price-and-cut algorithm. Dalmeijer and Spliet (2018) improve the results of Spliet and Gabor (2014) by introducing a novel class of valid inequalities for this problem. The VRP-TWA with time-dependent travel times is introduced in Spliet, Dabia, and Van Woensel (2017). Instead of fixed travel times, they assume that the arcs have time dependent travel times to take the daily pattern of morning and evening rush hours into account.

Subramanyam and Gounaris (2017) show that the time window assignment problem with uncertain demand can be reduced to the consistent vehicle routing problem (ConVRP) with arrival time consistency requirements. In this problem, every customer must be visited multiple times in a certain period and the difference between the earliest and latest arrival time at a customer must be lower than a certain constant. Using the branch-and-bound algorithm developed for the

ConVRP they are able to improve the results of Spliet and Gabor (2014). Their algorithm can also be used to consider uncertainty in travel times by constructing scenarios with different travel time perturbations.

Zhang et al. (2015) introduce the time window assignment problem for a maritime inventory routing problem. They look at a periodic setting in which the routes of the ships and the delivery time windows are a decision of the vendor. They take major disruptions of several days into account that result in several days delay on a route or at a port. The problem is formulated as a two-stage stochastic MIP and a two-phase solution approach is used in which first the routes are generated and second the time windows are allocated. In the routing phase, time buffers are inserted and the visits at a port are spread over the planning horizon. In the second phase, the time windows are assigned to every route by taking different disruption scenarios into account.

Jabali et al. (2015) introduce the vehicle routing problem with self imposed time windows (VRP-SITW) in which delivery time windows at the customers are imposed by a logistic service provider. They assume that an arc will suffer a delay with a certain probability and that the duration of the delay is a discrete random variable with known probability function. To reduce the number of scenarios they assume that exactly one arc in a solution will suffer a delay. The goal is to construct an a priori routing plan and time window assignment such that the travel time, lateness and overtime are minimized. An LP model is proposed to solve the time window assignment problem for a given route in which time buffers are allocated to customers to cope with possible delays. Estimates of this LP model are used in the proposed tabu search heuristic to solve the VRP-SITW. Vareias, Repoussis, and Tarantilis (2017) extend the work of Jabali et al. (2015) by allowing multiple arcs to be disrupted at the same time and by making the time window length a decision variable. They assume that the duration of a disruption at an arc is a continuous random variable with known distribution. The model is discretized by partitioning the total density function into parts of equal probability. Vareias, Repoussis, and Tarantilis (2017) propose a second model in which the uncertainty follows from the stochastic travel times that are modeled as a set of scenarios. The distribution of the arrival time at a customer is given by the Cartesian product formed by all possible scenarios used by the arcs traveled to reach the customer. For both models a mathematical model is proposed to solve the time window assignment problem for a given route. The objective of both models is to minimize the time window width, overtime and earliness and lateness at a customer. The VRP-TWA is solved by an adaptive large neighborhood search algorithm in which iteratively the routing problem and the time window assignment problem are solved.

Both the paper of Jabali et al. (2015) and Vareias, Repoussis, and Tarantilis (2017) solve a variant of the stochastic VRP-TWA and present a heuristic solution method. We propose a model for the robust VRP-TWA in which the travel times of the arcs are not completely known. To the

best of our knowledge, we are the first to tackle this problem. Furthermore, in our stochastic variant of the VRP-TWA, no scenarios or disruptions are assumed but the probability distribution of the travel time of every arc is assumed to be known. An exact solution method to solve simultaneously the routing and time window assignment problem for both the robust and stochastic VRP-TWA is proposed.

3. Problem description

The goal of the RVRP-TWA is to find an a priori routing solution and time window assignment that minimizes the risk of time window violations in terms of probability and magnitude of violations while the expected total travel time is kept below a certain threshold value, T.

To motivate the need for a robust solution method an example of a VRP-based routing solution and RVRP-TWA solution are presented in Figure 1. For the VRP-based solution, first the routing problem is solved and second the optimal time windows are determined for the final routing solution. In the RVRP-TWA the routing problem and time windows assignment are simultaneously solved as explained in Section 4 and 5. For this instance, the risk of violating the time windows of the RVRP-TWA solution is 36% lower than of the VRP-based solution while the travel time is only 4.3% higher.

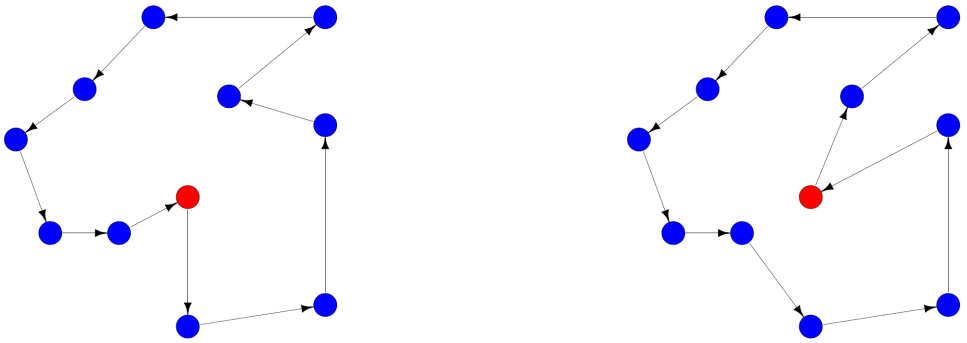

(a) VRP-based (b) RVRP-TWA

Figure 1 The route of the VRP-based solution approach and RVRP-TWA for an instance with 10 customers.

In this section, the feasible routing set is described and the RVRP-TWA is formally proposed. Throughout this chapter boldface lowercase characters are used to indicate a vector and tilde ($\tilde{\cdot}$) is used to denote an uncertain parameter.

3.1. Routing set

The RVRP-TWA is defined on a directed graph $G = (\mathcal{N}, \mathcal{A})$, with $\mathcal{N}$ the set of nodes and $\mathcal{A}$ the set of arcs. Let $\mathcal{K} = \{1, \ldots, K\}$ be the set of vehicles, then the set of nodes can be denoted by $\mathcal{N} = \{1, \ldots, n-1, n'_1, \ldots, n'_K, n\}$, with nodes 1 and n representing the depot and set $\mathcal{N}' = \{n'_1, n'_2, \ldots, n'_K\}$

representing the destination nodes of the vehicles. Similar to the notation used in Adulyasak and Jaillet (2016), the nodes in $\mathcal{N}'$ are copies of the depot node and all incoming arcs are the same. The end depot node n is only connected to the vehicle destination nodes, i.e., node n has K incoming arcs $(n'_k, n) \in \mathcal{A}$ with travel times equal to zero $\forall k \in \mathcal{K}$. We assume that all nodes $\mathcal{N}$ must be visited except for the destination nodes $\mathcal{N}'$.

Let $\mathcal{N}_T \subset \mathcal{N}$ be the set of nodes with an exogenous time window, defined by $[e_i, l_i]$ $\forall i \in \mathcal{N}_T$. To solve the time window assignment problem, an endogenous time window $[\tau_i, \tau_i + \epsilon_i] \subseteq [e_i, l_i]$ with start point τ_i and width ϵ_i has to be assigned to each node $i \in \mathcal{N}_T$. The start point of a time window τ_i is a decision variable and ϵ_i is a constant. The depot nodes 1 and n do not have a time window restriction, but the vehicle destination nodes $\mathcal{N}'$ have a fixed time window $[e_{n'_k}, l_{n'_k}] = [e_n, l_n]$ imposed. Hence, the endogenous time window of the vehicle destination nodes $\mathcal{N}'$ are equal to the exogenous time windows, i.e., $\tau_i = e_i$ and $\epsilon_i = l_i - e_i$ $\forall i \in \mathcal{N}'$.

We assume that the endogenous time windows are soft, i.e., if a vehicle arrives before or after the endogenous time window, the customer is immediately serviced. This is a reasonable assumption in our solution framework because (i) we enforce the expected arrival time at each customer to fall within the assigned time window (through the Slater's condition described in Section 4.1), and (ii) the risk measure considered in this framework is an exponential function which takes into account both the frequency and magnitude of the time window violations and thus routes which can potentially arrive much earlier or much later than the time window would be highly discouraged. Furthermore, we assume that the travel times are independent random variables. Let $\tilde{c}_a$ represent the uncertain travel time of arc $a \in \mathcal{A}$, with expected travel time c_a, minimum value $\underline{c}_a$ and maximum value $\bar{c}_a$. Jaillet, Qi, and Sim (2016) present a framework to deal with correlated travel times which can also be used in this setting as explained in Section 8. Furthermore, we assume fixed service times s_i, $i \in \mathcal{N}$, which are added to the travel time $\tilde{c}_a$ with $a = (i, j)$. Note that the method described in this chapter can also be used when the service times are random variables. In this case, $\forall i \in \mathcal{N} \backslash \mathcal{N}'$ a dummy node i' is created with only one incoming arc (i, i'), with travel time $\tilde{s}_i$.

To formulate the feasible routing set, the binary decision variables x_a and s_a^i are used. Variable x_a is one if arc a is used in the routing solution, otherwise zero, and s_a^i is equal to one if arc a is part of the route to node i. Variable z_i is equal to the number of times node $i \in \mathcal{N}$ is visited. For a given set of nodes $\mathcal{H} \subset \mathcal{N}$, let $\delta^-(\mathcal{H}) = \{(i, j) \in \mathcal{A} | i \in \mathcal{N} \backslash \mathcal{H}, j \in \mathcal{H}\}$ be the incoming arcs and

$\delta^+(\mathcal{H}) = \{(i, j) \in \mathcal{A} | i \in \mathcal{H}, j \in \mathcal{N} \backslash \mathcal{H}\}$ be the outgoing arcs. The capacity of every vehicle is Q and let $r(\mathcal{H})$ be the minimum number of vehicles needed to serve the nodes in set $\mathcal{H}$. The routing set, $\mathcal{S}$, is defined by

$$\mathcal{S} = \{(\mathbf{s}, \mathbf{x}, \mathbf{z}) | (1) - (14)\}$$

$$1 \leq z_i \leq K, \qquad \forall i = \{1, n\}, \tag{1}$$

$$z_i = 1, \qquad \forall i \in \mathcal{N} \backslash (\mathcal{N}' \cup \{1, n\}), \tag{2}$$

$$z_i \leq 1, \qquad \forall i \in \mathcal{N}', \tag{3}$$

$$\sum_{a \in \delta^-(i)} x_a = z_i, \qquad \forall i \in \mathcal{N} \backslash \{1\}, \tag{4}$$

$$\sum_{a \in \delta^+(i)} x_a = z_i, \qquad \forall i \in \mathcal{N} \backslash \{n\}, \tag{5}$$

$$\sum_{a \in \delta^+(1)} s_a^i = z_i, \qquad \forall i \in \mathcal{N}_T, \tag{6}$$

$$\sum_{a \in \delta^-(u)} s_a^i - \sum_{a \in \delta^+(u)} s_a^i = 0, \qquad \forall i \in \mathcal{N}_T, u \in \mathcal{N} \backslash \{1, i, n\}, \tag{7}$$

$$\sum_{a \in \delta^-(i)} s_a^i - \sum_{a \in \delta^+(i)} s_a^i = z_i, \qquad \forall i \in \mathcal{N}_T, \tag{8}$$

$$\sum_{a \in \mathcal{A}} c_a s_a^i \leq T, \tag{9}$$

$$\sum_{a \in \delta^+(\mathcal{H})} x_a \geq r(\mathcal{H}), \qquad \forall \mathcal{H} \subset \mathcal{N} \backslash \{1, n\} : |\mathcal{H}| \geq 2, \tag{10}$$

$$\sum_{a \in \mathcal{A}} c_a s_a^i \geq \sum_{a \in \mathcal{A}} c_a s_a^{i+1}, \qquad \forall i \in \mathcal{N}' \backslash \{n'_K\}, \tag{11}$$

$$0 \leq s_a^i \leq x_a, \qquad \forall i \in \mathcal{N}_T, \forall a \in \mathcal{A}, \tag{12}$$

$$z_i \in \mathbb{Z}^+, \qquad \forall i \in \mathcal{N}, \tag{13}$$

$$x_a \in \{0, 1\}, \qquad \forall a \in \mathcal{A}. \tag{14}$$

Constraints (1) ensure that the number of vehicles used does not exceed the number of vehicles available. Constraints (2) state that all customers must be visited and constraints (3) ensure that the vehicle destination nodes can be visited at most once. Constraints (4)-(5) are the arc flow conservation constraints. Constraints (6)-(8) ensure the flow balance for every route to node $i \in \mathcal{N}_T$. Every route should start at the origin (6) and the flow balance should hold at the intermediate nodes (7) and the final node (8). Constraint (9) ensures that the expected total travel time does not exceed the threshold value T. Constraints (10) are the capacity and subtour elimination constraints. To avoid identical routing solutions with a different numbering of the vehicles, the symmetry breaking constraints (11) are included. These ensure that the vehicles are numbered in order of decreasing expected travel time. Constraints (12) link the arc variables x_a and the route variables s_a^i, i.e., arc a can only be part of a route if this arc is traversed in the solution. Note that $\mathbf{s} = (\mathbf{s}^i)_{i \in \mathcal{N}_T}$, with $\mathbf{s}^i$ the binary solution vector representing the route to node i.

The length of the assigned endogenous time window and the travel time threshold value T are input parameters. To find the lowest value of threshold T, the VRP with the objective to minimize

average total travel time can be solved before addressing the RVRP-TWA. Let T_0 be this minimum expected total travel time, then the travel time threshold value T is set to $T = \rho T_0$ with $\rho > 1$.

3.2. RVRP-TWA problem formulation

In the RVRP-TWA, it is assumed that the exact distribution of the uncertain travel times $\tilde{\mathbf{c}}$ is unknown but it belongs to a family of distributions $\mathbb{F}$. In addition, the travel times are independent random variables, and therefore the arrival time at node i is given by $\tilde{t}_i = \tilde{\mathbf{c}}\mathbf{s}^{\mathrm{i}}$. To obtain a robust solution and to capture the risk of violating the endogenous time windows, the exponential disutility function introduced in Jaillet, Qi, and Sim (2016) will be used. Let $C_{\alpha_i}(\tilde{t}_i)$ be the deterministic value representing the worst case certainty equivalent of random arrival time $\tilde{t}_i$ at node i under risk tolerance parameter α_i. $C_{\alpha_i}(\tilde{t}_i)$ is defined as:

$$C_{\alpha_i}(\tilde{t}_i) = \begin{cases} \sup_{\mathbb{P}\in\mathbb{F}} \alpha_i \ln \mathbb{E}_{\mathbb{P}}\left(\exp\left(\frac{\tilde{t}_i}{\alpha_i}\right)\right) & \text{if } \alpha_i > 0 \\ \lim_{\beta\downarrow 0} C_\beta(\tilde{t}_i) & \text{if } \alpha_i = 0. \end{cases}$$

This function has some interesting properties that will be used in our solution method. In particular, Jaillet, Qi, and Sim (2016) show that $C_{\alpha_i}(\tilde{t}_i)$ is jointly convex in $(\alpha_i, \tilde{t}_i)$. The risk of violating the endogenous time window $[\tau_i, \tau_i + \epsilon_i]$ at node i is measured by the time window violation index defined by

$$\rho_{\tau_i} = \inf\{\alpha_i + \eta_i | C_{\alpha_i}(\tilde{t}_i) \le \tau_i + \epsilon_i, C_{\eta_i}(-\tilde{t}_i) \le -\tau_i\}.$$

This is the smallest risk tolerance such that the certainty equivalent of the arrival time does not exceed the lower and upper bound of the endogenous time window. Note that, $\rho_{\tau_i} = 0$ when the arrival time is guaranteed to meet the time window $[\tau_i, \tau_i + \epsilon_i]$ since α and η are both equal to zero. Furthermore, the time window violation index takes both the probability and the magnitude of the violation into account. More properties and details of the time window violation index are discussed in Appendix A.

The objective of the RVRP-TWA is to find the routing solution $\mathbf{s} \in \mathcal{S}$ and endogenous time windows $\boldsymbol{\tau}$ with the lowest time window violation index. Hence, the optimal route and time windows assignment can be found by solving the following optimization problem:

$$\inf \sum_{i\in\mathcal{N}_T} \alpha_i + \eta_i, \tag{15}$$

$$s.t.\ C_{\alpha_i}(\tilde{\mathbf{c}}\mathbf{s}^{\mathrm{i}}) \le \tau_i + \epsilon_i, \qquad \forall i \in \mathcal{N}_T, \tag{16}$$

$$C_{\eta_i}(-\tilde{\mathbf{c}}\mathbf{s}^{\mathrm{i}}) \le -\tau_i, \qquad \forall i \in \mathcal{N}_T, \tag{17}$$

$$e_i \le \tau_i \le l_i - \epsilon_i, \qquad \forall i \in \mathcal{N}_T, \tag{18}$$

$$\alpha_i, \eta_i \ge 0, \qquad \forall i \in \mathcal{N}_T, \tag{19}$$

$$\mathbf{s} \in \mathcal{S}. \tag{20}$$

The objective function (15) is to minimize the risk parameters. Constraints (16) and (17) ensure that the certainty equivalent of the arrival time does not exceed the bounds of the endogenous time window. The decision variables are presented in Constraints (18)-(20) in which Constraints (18) ensure that the endogenous time windows are included in the exogenous time windows.

4. Solution framework

Solving Problem (15)–(20) is challenging since function $C_{\alpha_i}()$ is nonlinear in α_i and the entire formulation with the routing set $\mathcal{S}$ is a mixed-integer non-linear program (MINLP). Therefore, we apply a decomposition technique to solve this problem. First, the subproblem of minimizing the time window violation index for a given routing solution $\mathbf{s} \in \mathcal{S}$ is investigated. If $\overline{\mathbf{cs}}^i - \underline{\mathbf{cs}}^i < \epsilon_i$ then α_i and η_i are both zero. Otherwise, the subproblem with objective value $f(\mathbf{s})$ is given by

$$f(\mathbf{s}) = \inf \sum_{i \in \mathcal{N}_T} \alpha_i + \eta_i, \tag{21}$$

$$s.t.\ C_{\alpha_i}(\tilde{\mathbf{cs}}^{\mathsf{i}}) \leq \tau_i + \epsilon_i, \qquad \forall i \in \mathcal{N}_T, \tag{22}$$

$$C_{\eta_i}(-\tilde{\mathbf{cs}}^{\mathsf{i}}) \leq -\tau_i, \qquad \forall i \in \mathcal{N}_T, \tag{23}$$

$$\max\{e_i, \underline{\mathbf{cs}}^i\} \leq \tau_i \leq \min\{l_i, \overline{\mathbf{cs}}^i\} - \epsilon_i, \qquad \forall i \in \mathcal{N}_T, \tag{24}$$

$$\alpha_i, \eta_i \geq 0, \qquad \forall i \in \mathcal{N}_T. \tag{25}$$

Constraints (24) ensure that the start time of the endogenous time window is not lower than the lowest possible arrival time $\underline{\mathbf{cs}}^i$, and the end time of the endogenous time window is not higher than the latest possible arrival time $\overline{\mathbf{cs}}^i$. Furthermore, the endogenous time windows are included in the exogenous time windows. Because C_{α_i} is convex in α_i, Problem (21)–(25) can be decomposed into $|\mathcal{N}_T|$ convex problems, each with three variables α_i, η_i and τ_i. Therefore, as stated in Proposition 1, $f(\mathbf{s})$ is a convex problem and the proof can be found in Appendix B.

PROPOSITION 1. *$f(\mathbf{s})$ is convex in $\mathbf{s}$*

Proposition 1 allows us to derive subgradient cuts from the solution of $f(s)$. In the next section, we focus on deriving the subgradient of $f(\mathbf{s})$ using the Lagrange function and we show that Benders decomposition can be used to solve the RVRP-TWA.

4.1. Derivation of the subgradient of $f(\mathbf{s})$

To guarantee feasibility of the problem, ϵ_i and the exogenous time window boundaries e_i, l_i $\forall i \in \mathcal{N}_T$, should be defined such that there exists a solution $\mathbf{s}$ for which the following conditions hold:

$$\lim_{\alpha_i \to \infty} C_{\alpha_i}(\tilde{\mathbf{cs}}^i) = \sup_{\mathbb{P} \in \mathbb{F}} \mathbb{E}_{\mathbb{P}}(\tilde{\mathbf{cs}}^i) \leq l_i, \qquad \forall i \in \mathcal{N}_T,$$

$$\lim_{\eta_i \to \infty} C_{\eta_i}(-\tilde{\mathbf{cs}}^i) = \sup_{\mathbb{P} \in \mathbb{F}} \mathbb{E}_{\mathbb{P}}(-\tilde{\mathbf{cs}}^i) \leq -e_i, \qquad \forall i \in \mathcal{N}_T,$$

$$\sup_{\mathbb{P} \in \mathbb{F}} (\mathbb{E}_{\mathbb{P}}(\tilde{\mathbf{cs}}^i) + \mathbb{E}_{\mathbb{P}}(-\tilde{\mathbf{cs}}^i)) < \epsilon_i, \qquad \forall i \in \mathcal{N}_T.$$

The first two conditions guarantee that the two worst cases of the expected arrival time at node i (early arrival and late arrival) are within the assigned time window. The third condition guarantees that the deviation between the two worst cases of the expected arrival time must be bounded by the time window size. These conditions ensure that the routing solution satisfy the time windows in expectation which is important in practice.

Hence, if these three conditions hold, then there exists a solution $\mathbf{s}$ and $\boldsymbol{\tau}$ for which

$$\begin{aligned}
&\lim_{\alpha_i \to \infty} C_{\alpha_i}(\tilde{\mathbf{c}}\mathbf{s}^i) = \sup_{\mathbb{P}\in\mathbb{F}} \mathbb{E}_{\mathbb{P}}(\tilde{\mathbf{c}}\mathbf{s}^i) \leq \tau_i + \epsilon_i, && \forall i \in \mathcal{N}_T,\\
&\lim_{\eta_i \to \infty} C_{\eta_i}(-\tilde{\mathbf{c}}\mathbf{s}^i) = \sup_{\mathbb{P}\in\mathbb{F}} \mathbb{E}_{\mathbb{P}}(-\tilde{\mathbf{c}}\mathbf{s}^i) \leq -\tau_i, && \forall i \in \mathcal{N}_T,\\
&e_i \leq \tau_i \leq l_i - \epsilon_i, && \forall i \in \mathcal{N}_T,
\end{aligned}$$

hold. Because C_{α_i} is monotonic decreasing in α_i, this implies that the Slater's condition is satisfied and therefore $f(\mathbf{s})$ is a classical convex problem. Strong duality implies that $f(\mathbf{s}) = \sup_{\boldsymbol{\lambda}\geq 0} \inf_{\boldsymbol{\alpha},\boldsymbol{\eta},\boldsymbol{\tau}\geq 0} L(\mathbf{s},\boldsymbol{\alpha},\boldsymbol{\eta},\boldsymbol{\tau},\boldsymbol{\lambda})$, with the Lagrange function given by

$$\begin{aligned}
L(\mathbf{s},\boldsymbol{\alpha},\boldsymbol{\eta},\boldsymbol{\tau},\boldsymbol{\lambda}) = &\sum_{i\in\mathcal{N}_T} \alpha_i + \sum_{i\in\mathcal{N}_T} \eta_i + \sum_{i\in\mathcal{N}_T} \overline{\lambda}(C_{\alpha_i}(\tilde{\mathbf{c}}\mathbf{s}^i) - \tau_i - \epsilon_i) + \sum_{i\in\mathcal{N}_T} \underline{\lambda}(C_{\eta_i}(-\tilde{\mathbf{c}}\mathbf{s}^i) + \tau_i)\\
&+ \sum_{i\in\mathcal{N}_T} \lambda_{1i}(e_i - \tau_i) + \sum_{i\in\mathcal{N}_T} \lambda_{2i}(\tau_i - l_i + \epsilon_i) + \sum_{i\in\mathcal{N}_T} \lambda_{3i}(\underline{\mathbf{c}}\mathbf{s}^i - \tau_i)\\
&+ \sum_{i\in\mathcal{N}_T} \lambda_{4i}(\tau_i - \overline{\mathbf{c}}\mathbf{s}^i + \epsilon_i).
\end{aligned}$$

Since L is linear in $\boldsymbol{\tau}$ and $C_{\alpha_i}(\tilde{\mathbf{c}}\mathbf{s}^i)$ is jointly convex in $(\alpha_i, \mathbf{s}^i)$ $\forall i \in \mathcal{N}_T$, the function $L(\mathbf{s},\boldsymbol{\alpha},\boldsymbol{\eta},\boldsymbol{\tau},\boldsymbol{\lambda})$ is jointly convex in $(\mathbf{s},\boldsymbol{\alpha},\boldsymbol{\eta},\boldsymbol{\tau})$, given $\boldsymbol{\lambda} \geq \mathbf{0}$. Based on strong duality we will show that the subgradient of function $f(\mathbf{s})$ is equal to the subgradient of function $L(\mathbf{s},\boldsymbol{\alpha},\boldsymbol{\eta},\boldsymbol{\tau},\boldsymbol{\lambda})$ with respect to $\mathbf{s}$.

$$\begin{aligned}
f(\mathbf{y}) - f(\mathbf{s}) = &\sup_{\boldsymbol{\lambda}\geq 0} \inf_{\boldsymbol{\alpha},\boldsymbol{\eta},\boldsymbol{\tau}\geq 0} L(\mathbf{y},\boldsymbol{\alpha},\boldsymbol{\eta},\boldsymbol{\tau},\boldsymbol{\lambda}) - \sup_{\boldsymbol{\lambda}\geq 0} \inf_{\boldsymbol{\alpha},\boldsymbol{\eta},\boldsymbol{\tau}\geq 0} L(\mathbf{s},\boldsymbol{\alpha},\boldsymbol{\eta},\boldsymbol{\tau},\boldsymbol{\lambda}) && (26)\\
\geq &\inf_{\boldsymbol{\alpha},\boldsymbol{\eta},\boldsymbol{\tau}\geq 0} L(\mathbf{y},\boldsymbol{\alpha},\boldsymbol{\eta},\boldsymbol{\tau},\boldsymbol{\lambda}^*) - \inf_{\boldsymbol{\alpha},\boldsymbol{\eta},\boldsymbol{\tau}\geq 0} L(\mathbf{s},\boldsymbol{\alpha},\boldsymbol{\eta},\boldsymbol{\tau},\boldsymbol{\lambda}^*) && (27)\\
= &L(\mathbf{y},\boldsymbol{\alpha}^y,\boldsymbol{\eta}^y,\boldsymbol{\tau}^y,\boldsymbol{\lambda}^*) - L(\mathbf{s},\boldsymbol{\alpha}^*,\boldsymbol{\eta}^*,\boldsymbol{\tau}^*,\boldsymbol{\lambda}^*) && (28)\\
\geq &d_s^L(\mathbf{s},\boldsymbol{\alpha}^*,\boldsymbol{\eta}^*,\boldsymbol{\tau}^*,\boldsymbol{\lambda}^*)(\mathbf{y}-\mathbf{s}) + d_\alpha^L(\mathbf{s},\boldsymbol{\alpha}^*,\boldsymbol{\eta}^*,\boldsymbol{\tau}^*,\boldsymbol{\lambda}^*)(\boldsymbol{\alpha}^y - \boldsymbol{\alpha}^*) + && (29)\\
&d_\eta^L(\mathbf{s},\boldsymbol{\alpha}^*,\boldsymbol{\eta}^*,\boldsymbol{\tau}^*,\boldsymbol{\lambda}^*)(\boldsymbol{\eta}^y - \boldsymbol{\eta}^*) + d_\tau^L(\mathbf{s},\boldsymbol{\alpha}^*,\boldsymbol{\eta}^*,\boldsymbol{\tau}^*,\boldsymbol{\lambda}^*)(\boldsymbol{\tau}^y - \boldsymbol{\tau}^*)\\
= &d_s^L(\mathbf{s},\boldsymbol{\alpha}^*,\boldsymbol{\eta}^*,\boldsymbol{\tau}^*,\boldsymbol{\lambda}^*)(\mathbf{y}-\mathbf{s}) && (30)
\end{aligned}$$

Note that $\boldsymbol{\lambda}^* = \arg\sup_{\boldsymbol{\lambda}\geq 0}(\inf_{\boldsymbol{\alpha},\boldsymbol{\eta},\boldsymbol{\tau}\geq 0} L(\mathbf{s},\boldsymbol{\alpha},\boldsymbol{\eta},\boldsymbol{\tau},\boldsymbol{\lambda}))$ in the first inequality (27) and let $(\boldsymbol{\alpha}^y,\boldsymbol{\eta}^y,\boldsymbol{\tau}^y) = \arg\inf_{\boldsymbol{\alpha},\boldsymbol{\eta},\boldsymbol{\tau}\geq 0} L(\mathbf{y},\boldsymbol{\alpha},\boldsymbol{\eta},\boldsymbol{\tau},\boldsymbol{\lambda}^*)$. Let $Z(\mathbf{s}) = \{(\boldsymbol{\alpha}^0,\boldsymbol{\eta}^0,\boldsymbol{\tau}^0,\boldsymbol{\lambda}^0) : L(\boldsymbol{\alpha}^0,\boldsymbol{\eta}^0,\boldsymbol{\tau}^0,\boldsymbol{\lambda}^0) = \sup_{\lambda\geq 0} \inf_{\alpha,\eta,\tau\geq 0} L(\mathbf{s},\boldsymbol{\alpha},\boldsymbol{\eta},\boldsymbol{\tau},\boldsymbol{\lambda})\}$, $(\boldsymbol{\alpha}^*,\boldsymbol{\eta}^*,\boldsymbol{\tau}^*,\boldsymbol{\lambda}^*) \in Z(S)$, and

$(d_s^L(\mathbf{s},\boldsymbol{\alpha^*},\boldsymbol{\eta^*},\boldsymbol{\tau^*},\boldsymbol{\lambda^*}), d_\alpha^L(\mathbf{s},\boldsymbol{\alpha^*},\boldsymbol{\eta^*},\boldsymbol{\tau^*},\boldsymbol{\lambda^*}), d_\eta^L(\mathbf{s},\boldsymbol{\alpha^*},\boldsymbol{\eta^*},\boldsymbol{\tau^*},\boldsymbol{\lambda^*}), d_\tau^L(\mathbf{s},\boldsymbol{\alpha^*},\boldsymbol{\eta^*},\boldsymbol{\tau^*},\boldsymbol{\lambda^*}))$
be the subgradient vector of function $L(\mathbf{s},\boldsymbol{\alpha},\boldsymbol{\eta},\boldsymbol{\tau},\boldsymbol{\lambda^*})$ at $(\mathbf{s},\boldsymbol{\alpha}^*,\boldsymbol{\eta}^*,\boldsymbol{\tau}^*)$. The second inequality follows from the fact that $L(\mathbf{s},\boldsymbol{\alpha},\boldsymbol{\eta},\boldsymbol{\tau},\boldsymbol{\lambda})$ is jointly convex in $(\mathbf{s},\boldsymbol{\alpha},\boldsymbol{\eta},\boldsymbol{\tau})$. Since $(\boldsymbol{\alpha}^*,\boldsymbol{\eta}^*,\boldsymbol{\tau}^*,\boldsymbol{\lambda}^*)\in Z(s)$, $d_{\boldsymbol{\alpha}}^L(\mathbf{s},\boldsymbol{\alpha^*},\boldsymbol{\eta^*},\boldsymbol{\tau^*},\boldsymbol{\lambda^*})=0$, $d_{\boldsymbol{\eta}}^L(\mathbf{s},\boldsymbol{\alpha^*},\boldsymbol{\eta^*},\boldsymbol{\tau^*},\boldsymbol{\lambda^*})=0$ and $d_\tau^L(\mathbf{s},\boldsymbol{\alpha^*},\boldsymbol{\eta^*},\boldsymbol{\tau^*},\boldsymbol{\lambda^*})=0$ and this shows that $d_s^L(\mathbf{s},\boldsymbol{\alpha^*},\boldsymbol{\eta^*},\boldsymbol{\tau^*},\boldsymbol{\lambda^*})$ is equal to the subgradient of $f(\mathbf{s})$.

For $i\in\mathcal{N}_T$ with $\alpha_i^*=\eta_i^*=0$, $\mathbf{s}^i$ is optimal, therefore the following equations hold

$$f(\mathbf{y}^i)-f(\mathbf{s}^i)=\alpha_i^y+\eta_i^y\geq d_{\mathbf{s}^i}^f(\mathbf{s})(\mathbf{y}^i-\mathbf{s}^i)\geq 0,\ \ \forall \mathbf{y}^i\in\mathcal{S}^i.$$

This implies that $d_{s_a^i}^f(\mathbf{s})=\mathbf{0}$ for all $a\in\mathcal{A}$.

Let $d_{s_a^i}^{c_1}(\alpha_i^*,\mathbf{s}^i)$ and $d_{s_a^i}^{c_2}(\eta_i^*,\mathbf{s}^i)$ be the subgradients of $C_{\alpha_i}(\tilde{\mathbf{c}}\mathbf{s}^i)$ and $C_{\eta_i}(-\tilde{\mathbf{c}}\mathbf{s}^i)$ with respect to s_a^i at point $(\alpha_i^*,\mathbf{s}^i)$ and $(\eta_i^*,\mathbf{s}^i)$, respectively. Derivating L along s_a^i, we obtain

$$d_{s_a^i}^L(\mathbf{s},\boldsymbol{\alpha^*},\boldsymbol{\eta^*},\boldsymbol{\tau^*},\boldsymbol{\lambda^*})=\overline{\lambda}^* d_{s_a^i}^{c_1}(\alpha_i^*,\mathbf{s}^i)+\underline{\lambda}^* d_{s_a^i}^{c_2}(\eta_i^*,\mathbf{s}^i)+\lambda_{3i}^*\underline{c}_a-\lambda_{4i}^*\overline{c}_a. \tag{31}$$

For $i\in\mathcal{N}_T$ with $\alpha_i^*\neq 0$ or $\eta_i^*\neq 0$, the KKT conditions are used to calculate the values of $\boldsymbol{\lambda}^*$ in equation (31). Since strong duality holds, the KKT conditions are sufficient to find the optimal solution. Therefore, $\boldsymbol{\alpha}^*$, $\boldsymbol{\eta}^*$ and $\boldsymbol{\tau}^*$ are optimal if and only if the KKT conditions, presented in (32)–(43), hold.

$$d_{\alpha_i}^L(\mathbf{s},\boldsymbol{\alpha^*},\boldsymbol{\eta^*},\boldsymbol{\tau^*},\boldsymbol{\lambda^*})=1+\overline{\lambda}^* d_{\alpha_i}^{c_1}(\alpha_i^*,\mathbf{s}^i)=0\Rightarrow\overline{\lambda}^*=\frac{-1}{d_{\alpha_i}^{c_1}(\alpha_i^*,\mathbf{s}^i)} \tag{32}$$

$$d_{\eta_i}^L(\mathbf{s},\boldsymbol{\alpha^*},\boldsymbol{\eta^*},\boldsymbol{\tau^*},\boldsymbol{\lambda^*})=1+\underline{\lambda}^* d_{\eta_i}^{c_2}(\eta_i^*,\mathbf{s}^i)=0\Rightarrow\underline{\lambda}^*=\frac{-1}{d_{\eta_i}^{c_2}(\eta_i^*,\mathbf{s}^i)} \tag{33}$$

$$d_{\tau_i}^L(\mathbf{s},\boldsymbol{\alpha^*},\boldsymbol{\eta^*},\boldsymbol{\tau^*},\boldsymbol{\lambda^*})=\underline{\lambda}^*-\overline{\lambda}^*-\lambda_{1i}^*+\lambda_{2i}^*-\lambda_{3i}^*+\lambda_{4i}^*=0 \tag{34}$$

$$\overline{\lambda}^*(C_{\alpha_i^*}(\tilde{\mathbf{c}}\mathbf{s}^i)-\tau_i^*-\epsilon_i)=0 \tag{35}$$

$$\underline{\lambda}^*(C_{\eta_i^*}(-\tilde{\mathbf{c}}\mathbf{s}^i)+\tau_i^*)=0 \tag{36}$$

$$\lambda_{1i}^*(e_i-\tau_i^*)=0 \tag{37}$$

$$\lambda_{2i}^*(\tau_i^*-l_i+\epsilon_i)=0 \tag{38}$$

$$\lambda_{3i}^*(\underline{\mathbf{c}}\mathbf{s}^i-\tau_i^*)=0 \tag{39}$$

$$\lambda_{4i}^*(\tau_i^*-\overline{\mathbf{c}}\mathbf{s}^i+\epsilon_i)=0 \tag{40}$$

$$C_{\alpha_i^*}(\tilde{\mathbf{c}}\mathbf{s}^i)\leq\tau_i^*+\epsilon_i \tag{41}$$

$$C_{\eta_i^*}(-\tilde{\mathbf{c}}\mathbf{s}^i)\geq-\tau_i^* \tag{42}$$

$$\min\{e_i,\underline{\mathbf{c}}\mathbf{s}^i\}\leq\tau_i^*\leq\max\{l_i,\overline{\mathbf{c}}\mathbf{s}^i\}-\epsilon_i. \tag{43}$$

If $\alpha_i\neq 0$ or $\eta_i\neq 0$ then $C_{\alpha_i^*}(\tilde{\mathbf{c}}\mathbf{s}^i)=\tau_i^*+\epsilon_i$ and $C_{\eta_i^*}(-\tilde{\mathbf{c}}\mathbf{s}^i)=-\tau_i^*$ to keep α_i and η_i as low as possible. Otherwise the objective can be improved by increasing the time window length. Using

equations (32) and (33), we get $\overline{\lambda}^* = \frac{-1}{d^{c_1}_{\alpha_i}(\alpha_i^*, \mathbf{s}^i)}$ and $\underline{\lambda}^* = \frac{-1}{d^{c_2}_{\eta_i}(\eta_i^*, \mathbf{s}^i)}$. If τ_i^* is not bounded by the lower or upper bound, i.e., if $\min\{e_i, \underline{\mathbf{c}}\mathbf{s}^i\} < \tau_i^* < \max\{l_i, \overline{\mathbf{c}}\mathbf{s}^i\} - \epsilon_i$ then $\lambda_{1i}^* = \lambda_{2i}^* = \lambda_{3i}^* = \lambda_{4i}^* = 0$ and $\alpha_i^*, \eta_i^* > 0$. Following equation (34) this means that $\overline{\lambda}^* = \underline{\lambda}^*$, so $d^{c_1}_{\alpha_i}(\alpha_i^*, \mathbf{s}^i) = d^{c_2}_{\eta_i}(\eta_i^*, \mathbf{s}^i)$. If τ_i^* is bounded by $e_i, l_i - \epsilon_i, \underline{\mathbf{c}}\mathbf{s}^i$, or $\overline{\mathbf{c}}\mathbf{s}^i - \epsilon_i$ then the corresponding $\lambda_{1i}^*, \lambda_{2i}^*, \lambda_{3i}^*$, or λ_{4i}^* is nonzero. For example, if $\tau_i^* = \underline{\mathbf{c}}\mathbf{s}^i$ then $\lambda_{3i}^* = \underline{\lambda}^* - \overline{\lambda}^*$ to ensure that equation (34) is equal to zero. Furthermore, a vehicle cannot arrive before $\underline{\mathbf{c}}\mathbf{s}^i$, so if $\tau_i = \underline{\mathbf{c}}\mathbf{s}^i$ then $\eta_i = 0$, similarly if $\tau_i = \overline{\mathbf{c}}\mathbf{s}^i - \epsilon_i$ then $\alpha_i = 0$. Therefore, the subgradient of $f(\mathbf{s})$ with respect to s_a^i can be calculated by:

$$d^f_{s_a^i}(\mathbf{s}) = \begin{cases} \overline{\lambda}^* d^{c_1}_{s_a^i}(\alpha_i^*, \mathbf{s}^i) + \underline{\lambda}^* d^{c_2}_{s_a^i}(\eta_i^*, \mathbf{s}^i) & \alpha_i^*, \eta_i^* > 0. \\ \overline{\lambda}^* d^{c_1}_{s_a^i}(\alpha_i^*, \mathbf{s}^i) + \underline{\lambda}^* d^{c_2}_{s_a^i}(\eta_i^*, \mathbf{s}^i) + (\underline{\lambda}^* - \overline{\lambda}^*)\underline{c}_a & \alpha_i^* > 0, \eta_i^* = 0 \\ \overline{\lambda}^* d^{c_1}_{s_a^i}(\alpha_i^*, \mathbf{s}^i) + \underline{\lambda}^* d^{c_2}_{s_a^i}(\eta_i^*, \mathbf{s}^i) + (\underline{\lambda}^* - \overline{\lambda}^*)\overline{c}_a & \alpha_i^* = 0, \eta_i^* > 0 \\ 0 & \alpha_i^* = \eta_i^* = 0 \end{cases} \tag{44}$$

with $\overline{\lambda}^* = \frac{-1}{d^{c_1}_{\alpha_i}(\alpha_i^*, \mathbf{s}^i)}$ and $\underline{\lambda}^* = \frac{-1}{d^{c_2}_{\eta_i}(\eta_i^*, \mathbf{s}^i)}$. The details of the computation of the subgradients $d^{c_1}_{s_a^i}(\alpha_i^*, \mathbf{s}^i)$, $d^{c_2}_{s_a^i}(\eta_i^*, \mathbf{s}^i)$, $d^{c_1}_{\alpha_i}(\alpha_i^*, \mathbf{s}^i)$ and $d^{c_2}_{\eta_i}(\eta_i^*, \mathbf{s}^i)$ are given in Appendix A. Using derivative (44), the RVRP-TWA model (15)–(20) can be reformulated as

$$\inf\ w, \tag{45}$$

$$\text{s.t. } f(\mathbf{p}) + d^f_p(\mathbf{p})(\mathbf{s} - \mathbf{p}) \le w, \qquad \forall \mathbf{p} \in \mathcal{S}, \tag{46}$$

$$\sum_{a \in \mathcal{A}} \sup_{p \in \mathbb{F}} \mathbb{E}(\tilde{c}_a) s_a^i \le l_i, \qquad \forall i \in \mathcal{N}_T, \tag{47}$$

$$\sum_{a \in \mathcal{A}} \sup_{p \in \mathbb{F}} \mathbb{E}(-\tilde{c}_a) s_a^i \le e_i, \qquad \forall i \in \mathcal{N}_T, \tag{48}$$

$$\sum_{a \in \mathcal{A}} (\sup_{p \in \mathbb{F}} \mathbb{E}(\tilde{c}_a) - \sup_{p \in \mathbb{F}} \mathbb{E}(-\tilde{c}_a)) s_a^i \le \epsilon_i, \qquad \forall i \in \mathcal{N}_T, \tag{49}$$

$$\mathbf{s} \in \mathcal{S}. \tag{50}$$

Constraints (47)–(49) ensure that the solution is feasible. Problem (46)–(50) is solved using a branch-and-cut approach described in Section 5. Since the routing set $\mathcal{S}$ is exponential in size, the subgradient cuts (46) are added in a branch-and-cut fashion.

4.2. Time window assignment for a given route

To solve Problem (45)–(50), an efficient way to determine the optimal time window assignment for a routing solution is needed. Therefore, in this section a method is proposed to efficiently determine the optimal values of $\boldsymbol{\alpha}$, $\boldsymbol{\eta}$ and $\boldsymbol{\tau}$ for a given routing solution $\mathbf{s}$. If $\overline{\mathbf{c}}\mathbf{s}^i - \underline{\mathbf{c}}\mathbf{s}^i \le \epsilon$, then $\tau_i = \underline{\mathbf{c}}\mathbf{s}^i$ is optimal since $\alpha_i = 0$ and $\eta_i = 0$. Otherwise if $\overline{\mathbf{c}}\mathbf{s}^i - \underline{\mathbf{c}}\mathbf{s}^i > \epsilon$ and $\min\{e_i, \underline{\mathbf{c}}\mathbf{s}^i\} < \tau_i^* < \max\{l_i, \overline{\mathbf{c}}\mathbf{s}^i\} - \epsilon_i$, then we know from the KKT conditions that the optimal values α_i^*, η_i^*, and τ_i^* should satisfy the following three conditions:

1. $C_{\alpha_i^*}(\tilde{\mathbf{c}}\mathbf{s}^i) = \tau_i^* + \epsilon_i$
2. $C_{\eta_i^*}(-\tilde{\mathbf{c}}\mathbf{s}^i) = -\tau_i^*$
3. $d^{c1}_{\alpha_i}(\alpha_i^*, \mathbf{s}^i) = d^{c2}_{\eta_i}(\eta_i^*, \mathbf{s}^i)$

The first and second condition ensure that the values of α_i and η_i are as low as possible. The third condition implies that the objective cannot be improved, since both derivatives are equal, i.e., decreasing α_i will increase η_i with the same value. This condition only holds if τ_i^* is not equal to a boundary point, i.e., $\tau_i^* \neq e_i, \underline{\mathbf{c}}\mathbf{s}^i, l_i - \epsilon_i, \overline{\mathbf{c}}\mathbf{s}^i - \epsilon_i$. Since then $\lambda_k = 0$ for each k and $\overline{\lambda}^* = \underline{\lambda}^*$. In the proposed approach, initial checks are performed such that the boundary case is also covered.

The above three conditions will be used to efficiently solve Problem (21)-(25), i.e., to find the optimal values of α_i, η_i and τ_i for route $\mathbf{s}^i$. Figure 2 illustrates how the optimal value of τ_i can be found for a simple example in which the route to customer i consists of a single arc $a = (0, i)$. Let $\tilde{c}_a$ be the travel time of this arc with $\mathbb{F} = \{\mathbb{E}_{\mathbb{P}}(\tilde{c}_a) = 10, \mathbb{P}(\tilde{c}_a \in [7, 15]) = 1\}$. Note that the arrival time at customer i is $\tilde{t}_i = \tilde{c}_a$, since the route consists only of arc a. In the left graph, examples of the functions $C_{\alpha_i}(\tilde{t}_i)$ and $-C_{\eta_i}(-\tilde{t}_i)$ are given. In the right graph, the derivatives of $C_{\alpha_i}(\tilde{t}_i)$ and $C_{\eta_i}(-\tilde{t}_i)$ with respect to α_i and η_i are shown for different values of τ_i. When shifting graph $d^{c1}_{\alpha_i}$ by ϵ_i units to the left, the crosspoint of this shifted graph with graph $d^{c2}_{\eta_i}$ represents the optimal value of τ_i, i.e., all three conditions hold at this crosspoint. The optimal values corresponding to Figure 2 are $\tau_i^* = 8.5$, $\alpha_i^* = 5.2$ and $\eta_i^* = 3.7$ given that $\epsilon_i = 3$.

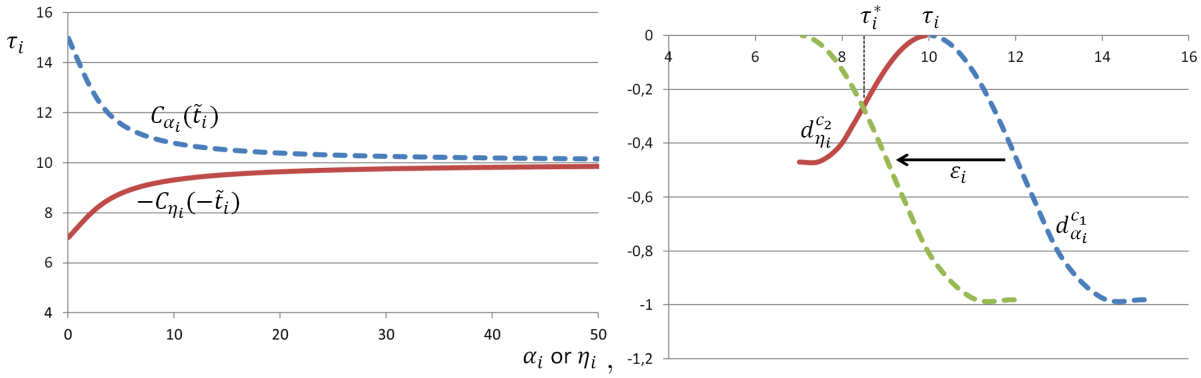

Figure 2 **The left graph shows examples of $C_{\alpha_i}(\tilde{t}_i)$ and $-C_{\eta_i}(-\tilde{t}_i)$ and the right graph shows the derivative of these function with respect to α_i and η_i, respectively.**

A variant of the binsearch algorithm is used to quickly determine this crosspoint. Instead of performing the binsearch algorithm on only one variable, it was performed on both τ_i and the derivative value d^c. The lower and upper bound of the derivative are initialized by $d_{lb} = -\infty$ and $d_{ub} = 0$, respectively. At every iteration, the variable with the smallest remaining solution space is chosen and the midpoint of this solution space is selected as target value. Before starting the search, checks were carried out to see if a crosspoint exists between $\tau_{lb} = \max\{e_i, \underline{\mathbf{c}}\mathbf{s}^i\}$ and $\tau_{ub} =$

$\min\{l_i, \overline{\mathbf{c}}\mathbf{s}^i\} - \epsilon_i$, otherwise the optimal value of τ_i is equal to one of these boundary points and we are done. The pseudo-code of this algorithm is given in Algorithm 1.

Algorithm 1 Calculation optimal τ_i^*

1: Initialize: $\tau_i = \mathbf{cs}^i - \epsilon_i/2$, $\tau_{lb} = \max\{e_i, \underline{\mathbf{c}}\mathbf{s}^i\}$, $\tau_{ub} = \min\{l_i, \overline{\mathbf{c}}\mathbf{s}^i\} - \epsilon_i$, $d_{lb} = 0$ and $d_{ub} = -\infty$
2: **if** no crosspoint inside τ_{lb} and τ_{ub} **then**
3: return $\tau_i^* = \tau_{lb}$ or $\tau_i^* = \tau_{ub}$
4: **end if**
5: Calculate α_i and η_i using binsearch, s.t. $C_{\alpha_i}(t_i) = \tau_i + \epsilon$ and $C_{\eta_i}(-t_i) = -\tau_i$
6: Calculate the corresponding derivative values $dC_\alpha = d^{c_1}_{\alpha_i}(\alpha_i, \mathbf{s}^i)$ and $dC_\eta = d^{c_2}_{\eta_i}(\eta_i, \mathbf{s}^i)$
7: *Update lower and upper bounds:*
8: **if** $dC_\alpha < dC_\eta$ **then**
9: $d_{lb} = \max\{d_{lb}, dC_\alpha\}$, $d_{ub} = \min\{d_{ub}, dC_\eta\}$, $\tau_{ub} = \tau_i$
10: **else**
11: $d_{lb} = \max\{d_{lb}, dC_\eta\}$, $d_{ub} = \min\{d_{ub}, dC_\alpha\}$, $\tau_{lb} = \tau_i$
12: **end if**
13: **while** $\tau_{ub} - \tau_{lb} > \varepsilon$ & $d_{ub} - d_{lb} > \varepsilon$ **do**
14: **if** $d_{ub} - d_{lb} < \tau_{ub} - \tau_{lb}$ **then**
15: $d = (d_{ub} - d_{lb})/2$
16: Calculate the α_i and η_i using binsearch, s.t. $d^{c_1}_{\alpha_i}(\alpha_i, \mathbf{s}^i) = d^{c_2}_{\eta_i}(\eta_i, \mathbf{s}^i) = d$
17: Calculate the corresponding τ_i values, s.t. $\tau_\alpha = C_{\alpha_i}(t_i) - \epsilon_i$ and $\tau_\eta = -C_{\eta_i}(-t_i)$
18: *Update lower and upper bounds:*
19: **if** $\tau_\eta < \tau_\alpha$ **then**
20: $\tau_{lb} = \max\{\tau_{lb}, \tau_\eta\}$, $\tau_{ub} = \min\{\tau_{ub}, \tau_\alpha\}$, $d_{lb} = d$
21: **else**
22: $\tau_{lb} = \max\{\tau_{lb}, \tau_\alpha\}$, $\tau_{ub} = \min\{\tau_{ub}, \tau_\eta\}$, $d_{ub} = d$
23: **end if**
24: **else**
25: $\tau_i = (\tau_{ub} - \tau_{lb})/2$
26: Calculate α_i and η_i using binsearch, s.t. $C_\alpha(t) = \tau_i + \epsilon$ and $C_\eta(-t) = -\tau_i$
27: Calculate the corresponding derivative values $dC_\alpha = d^{c_1}_{\alpha_i}(\alpha_i, \mathbf{s}^i)$ and
28: $dC_\eta = d^{c_2}_{\eta_i}(\eta_i, \mathbf{s}^i)$
29: Update lower and upper bounds as in lines 8–12
30: **end if**
31: **end while**
32: return $\tau_i^* = (\tau_{lb} + \tau_{ub})/2$

5. Branch-and-cut algorithm

Problem (45)–(50) is solved using a branch-and-cut algorithm. The subtour elimination constraints (10) and the subgradient cuts (46) are added during the branch-and-bound process. When a solution at a branch-and-bound node violates the subtour elimination constraint, the violated constraint is added and the problem of the current node is resolved. This process continues until no more constraints are violated. To detect and generate the violated subtour elimination constraints, the separation procedure of Lysgaard, Letchford, and Eglese (2004) for the VRP is used. The subgradient cuts (46) are derived from feasible integer routing solutions. When a feasible solution is found in the branch-and-bound tree, the corresponding cut is generated and added to the problem.

The subgradient cuts (46) constrain the risk of an entire solution $\mathbf{p} \in \mathcal{S}$. To strengthen the lower bound, risk cuts for individual customers are added. Let $\mathcal{A}^i_{\mathrm{p}} = \{a \in \mathcal{A} | p^i_a = 1\}$ be the set of arcs that are part of the route to customer i and let w^{p}_i be the time window violation index encountered at customer $i \in \mathcal{N}_T$ in solution $\mathbf{p} \in \mathcal{S}$. The total time window violation index w can be decomposed in $w = \sum_{i \in \mathcal{N}_T} w_i$, with w_i the index of customer i. Next to the subgradient cuts (46), the following cuts are added to Model (45)–(50) for every feasible integer solution $\mathbf{p} \in \mathcal{S}$ found in the branch-and-bound tree:

$$w^{\mathrm{p}}_i + \sum_{a \in \mathcal{A}^i_{\mathrm{p}}} w^{\mathrm{p}}_i (s^i_a - p^i_a) \leq w_i \quad \forall i \in \mathcal{N}_T, \forall \mathbf{p} \in \mathcal{S} \tag{51}$$

The left hand side of Constraint (51) is equal to w^{p}_i if the solution vector $\mathbf{s}^i$ is equal to or contains $\mathbf{p}^i$, i.e., if $\mathcal{A}^i_{\mathrm{p}} \subseteq \mathcal{A}^i_{\mathrm{s}}$. Otherwise, the left hand side is negative.

6. Stochastic VRP-TWA

The objective of the Stochastic VRP-TWA (SVRP-TWA) is to minimize the expected time window violation while ensuring that the expected total travel time is below a certain threshold value, T. In the SVRP-TWA, the probability distributions of the travel times are assumed to be known. Let $\tilde{t}_i$ be the uncertain arrival time variable at node i. Suppose that for a given solution $\mathbf{s}$, the arrival time density function at node i is given by $f^{\mathrm{s}}_{t_i}$, then for time window assignment $\boldsymbol{\tau}$ the expected time window violation at node i is given by

$$\beta^i_{\mathrm{s}}(\tau_i) = \int_{-\infty}^{\tau_i} (\tau_i - x) f^{\mathrm{s}}_{t_i}(x) dx + \int_{\tau_i + \epsilon_i}^{\infty} (x - \tau_i - \epsilon_i) f^{\mathrm{s}}_{t_i}(x) dx.$$

The optimal time window assignment for node i in solution $\mathbf{s}$ can be found by solving $\beta^i_{\mathrm{s}} = \min_{\tau_i \in [e_i, l_i - \epsilon_i]} \beta^i_s(\tau_i)$, with β^i_{s} the minimum expected time window violation for routing solution $s \in \mathcal{S}$. The optimal value of τ_i can be found by solving:

$$\frac{\partial}{\partial \tau_i} \left(\int_{-\infty}^{\tau_i} (\tau_i - x) f^{\mathrm{s}}_{t_i}(x) dx + \int_{\tau_i + \epsilon_i}^{\infty} (x - \tau_i - \epsilon_i) f^{\mathrm{s}}_{t_i}(x) dx \right) = 0 \tag{52}$$

$$\Rightarrow \int_{-\infty}^{\tau_i} f^{\mathrm{S}}_{t_i}(x)dx - \int_{\tau_i+\epsilon_i}^{\infty} f^{\mathrm{S}}_{t_i}(x)dx = 0 \tag{53}$$

$$\Rightarrow F^{\mathrm{S}}_{t_i}(\tau_i) = 1 - F^{\mathrm{S}}_{t_i}(\tau_i + \epsilon_i). \tag{54}$$

The Leibniz integral rule is used to obtain equation (53) and $F^s_{t_i}$ is the cumulative distribution function. Since $f^{\mathrm{S}}_{t_i}$ is positive, the second derivative of β^s_i is positive, i.e., $f^s_{t_i}(\tau_i) + f^s_{t_i}(\tau_i + \epsilon_i) \geq 0$. Therefore, the value τ^*_i resulting from solving equation (54) is the global minimum. Hence, for the optimal value τ^*_i, the probability of arriving before the start of the time window (τ^*_i) is equal to the probability of arriving after the closing time of the time window ($\tau^*_i + \epsilon_i$).

In the SVRP-TWA, the goal is to find the routing solution $\mathbf{s} \in \mathcal{S}$ that minimizes $\sum_{i \in \mathcal{N}_T} \beta^i_{\mathrm{S}}$. Hence, the stochastic model is defined by $\min_{\mathrm{S} \in \mathcal{S}} \sum_{i \in \mathcal{N}_T} \beta^i_s$. Since it is computational intensive to calculate $\beta^i_s \ \forall i \in \mathcal{N}_T$ for all solutions $\mathbf{s} \in \mathcal{S}$, the problem has been reformulated as follows:

$$\inf \sum_{i \in \mathcal{N}_T} v_i, \tag{55}$$

$$\text{s.t. } \beta^i_{\mathrm{P}} + \sum_{a \in \mathcal{A}^i_{\mathrm{P}}} \beta^i_{\mathrm{P}}(s^i_a - 1) \leq v_i, \qquad \forall i \in \mathcal{N}_T, \forall \mathbf{p} \in \mathcal{S}, \tag{56}$$

$$v_i \geq 0, \qquad \forall i \in \mathcal{N}_T, \tag{57}$$

$$\mathbf{s} \in \mathcal{S}. \tag{58}$$

The left hand side of Constraint (56) takes the value β^i_{P} if the arcs that are part of solution $\mathbf{p}^i$ are also contained in solution $\mathbf{s}^i$, i.e., if $\mathcal{A}^i_{\mathrm{P}} = \mathcal{A}^i_{\mathrm{S}}$, otherwise it takes a negative value. Similar to the subgradient cuts (46), Constraints (56) are added in a branch-and-cut fashion.

Note that the time window violation index could also be used in the stochastic model. In this case, the supremum term would disappear and the expected value in $\alpha_i \ln \mathbb{E}(\exp(\tilde{t}_i/\alpha_i))$ could be calculated by a sampling based approach. However, in the stochastic setting the distribution is known, therefore, the expected time window violation can be calculated directly and the time window violation index is not needed to measure the risk.

6.1. Sampling based approach

For some commonly used travel time distributions, e.g., independent normal or gamma distributed travel times (Ehmke, Campbell, and Urban 2015, Taş et al. 2013), the arrival time distribution is easy to calculate, and thus Equation (54) can be easily solved. However, in many cases it will be difficult to calculate the exact arrival time distribution $f^{\mathrm{S}}_{t_i}$. A common approach to calculate β^i_{S}, is to perform a Monte Carlo sampling approach in which a set of scenarios of the travel time vector $\tilde{\mathbf{c}}$ are generated. Let Ω be the set of scenarios and let $t^1_i, \ldots, t^{|\Omega|}_i$ be the corresponding arrival times

at node i for solution $\mathbf{s}$. It is assumed that τ_i is an integer, e.g., representing minutes. The optimal value of τ_i can be determined by solving

$$\min_{\tau_i \in [e_i, l_i - \epsilon_i]} \tilde{\beta}^i_{\mathrm{S}}(\tau_i) = \min_{\tau_i \in [e_i, l_i - \epsilon_i]} \frac{1}{|\Omega|} \sum_{\omega \in \Omega} |\min\{t^\omega_i - \tau_i, \tau_i + \epsilon_i - t^\omega_i, 0\}|. \tag{59}$$

In this sampling approach, $\tilde{\beta}^i_{\mathrm{S}}(\tau_i)$ represents the average violation of time window $[\tau_i, \tau_i + \epsilon_i]$ at node $i \in \mathcal{N}_T$ in solution $\mathbf{s}$ and can be used in Constraint (56). Note that $|\min\{t^\omega_i - \tau_i, \tau_i + \epsilon_i - t^\omega_i, 0\}|$ is a piece-wise linear convex function with respect to τ_i. Thus, $\tilde{\beta}^i_{\mathrm{S}}(\tau_i)$ is a piece-wise linear convex function and, therefore, only one search direction $\tilde{\beta}^i_{\mathrm{S}}(\tau^*_i + 1)$ or $\tilde{\beta}^i_{\mathrm{S}}(\tau^*_i - 1)$ can lead to an improvement of $\tilde{\beta}^i_{\mathrm{S}}(\tau^*_i)$. This is used in Algorithm 2 to determine the optimal value of τ_i, i.e., to solve Equation (59).

Algorithm 2 Determine optimal value τ^*_i

Initialize $\tau^*_i = \min\{\max\{e_i, \frac{1}{|\Omega|}\sum_{\omega \in \Omega} t^\omega_i - \frac{\epsilon_i}{2}\}, l_i - \epsilon_i\}$
if $\tilde{\beta}^i_{\mathrm{S}}(\tau^*_i + 1) < \tilde{\beta}^i_{\mathrm{S}}(\tau^*_i)$ **then**
    while $\tilde{\beta}^i_{\mathrm{S}}(\tau^*_i + 1) < \tilde{\beta}^i_{\mathrm{S}}(\tau^*_i)$ & $\tau^*_i + 1 \leq l_i - \epsilon_i$ **do**
        $\tau^*_i = \tau^*_i + 1$
    end while
else
    while $\tilde{\beta}^i_{\mathrm{S}}(\tau^*_i - 1) < \tilde{\beta}^i_{\mathrm{S}}(\tau^*_i)$ & $\tau^*_i - 1 \geq e_i$ **do**
        $\tau^*_i = \tau^*_i - 1$
    end while
end if

7. Results

Various computational experiments are performed to evaluate the performance of the proposed algorithms. All algorithms are implemented in C# under Windows 7 using CPLEX 12.8.0. The experiments are performed on a single core of a workstation with a 2.1 GHz Intel Core E5-2683 v4 processor and 128GB of RAM. The maximum running time is set to two hours. Unless stated otherwise, the following parameter settings are used. The time window length is set to 30 minutes for all customers, i.e., $\epsilon_i = \hat{\epsilon} = 30 \ \forall i \in \mathcal{N}_T$. The exogenous time window is set to nine hours for all nodes $i \in \mathcal{N}_T$. The average total travel time can increase with maximum 5% compared to the minimal expected total travel time T_0, i.e., $\rho = 1.05$. Furthermore, we assume that a time window has to be assigned to all customers, i.e., $\mathcal{N}_T = \mathcal{N} \backslash \{1, n\}$.

7.1. Instances

As shown in Jaillet, Qi, and Sim (2016), the computational time of their algorithm using the binary variables s_a^i, is very sensitive to the number of arcs. Jaillet, Qi, and Sim (2016) and Adulyasak and Jaillet (2016) use instances with $3n$ arcs that were randomly selected. As a result, in many of their instances there is only a single feasible routing solution with an expected total travel time below $1.1T_0$ (i.e., 10% above the optimal expected total travel time based on the VRP solution), which makes their instances not useful to examine the trade-off between the risk and expected total travel time of various routing solutions. Therefore, we generated new instances for the RVRP-TWA based on the Solomon (1987) instances and an arc selection method is proposed to reduce the number of arcs.

7.1.1. RVRP-TWA instances generation

In the RVRP-TWA, the mean, minimum, and maximum travel time of each arc is known. To compare the results of the RVRP-TWA with the results of the SVRP-TWA, we based these characteristics on specific distributions. In particular, instances based on triangular and shifted gamma distributed travel times were generated, since these distributions are often assumed in the stochastic VRP (Taş et al. 2013, Adulyasak and Jaillet 2016, Vareias, Repoussis, and Tarantilis 2017). The first three instance sets (T1, T2, T3) are made using the triangular distribution, characterized by a minimum value $\underline{c}_a$, a maximum value $\overline{c}_a$ and a mode m_a. Let u_a be the Euclidean distance of arc $a \in \mathcal{A}$ then the minimum value of the travel time of this arc is randomly drawn from the interval $\underline{c}_a \in [0.8u_a, 1.2u_a]$, and similarly $\overline{c}_a \in [1.25u_a, 2.5u_a]$. The T1 instances are symmetric with mode $m_a = \frac{\underline{c}_a + \overline{c}_a}{2}$ and the T2 and T3 instances are right skewed with $m_a = \underline{c}_a + \frac{\overline{c}_a - \underline{c}_a}{4}$ and $m_a = \underline{c}_a$, respectively. The mean travel time needed in the robust approach is calculated by $c_a = \frac{\underline{c}_a + \overline{c}_a + m_a}{3}$. Instance sets G1, G2 and G3 are based on the shifted gamma distribution and they are characterized by the shape parameter α and the rate parameter λ. For every arc $a \in \mathcal{A}$, parameters α_a and λ_a are randomly drawn from the intervals in Table 1. Let $G(0.01)$ be the inverse cumulative gamma distribution with probability 0.01. The travel time distribution of arc a is equal to the gamma distribution shifted $u_a - G(0.01)$ to the right. Therefore the characteristics of the travel time of arc a is given by $\underline{c}_a = u_a$, $\overline{c}_a = u_a - G(0.01) + G(0.99)$ and $c_a = \alpha_a \lambda_a$. Note that the α and λ values in Table 1 are generated such that the average difference between the maximum and minimum travel time of an arc is between 16.2 and 17.2 for G1, G2 and G3. For the triangular instances the minimum and maximum values are the same for the three instance sets T1, T2 and T3.

Per instance set, six different instances were generated based on the Solomon (1987) instances. To ensure feasible solutions with a finite time window violations index, the exogenous time window of every customer and the depot (planning horizon) are each set to nine hours. Since the time

instance	α	λ
G1	$[5, 20]$	1
G2	$[2, 3]$	$[1.5, 3]$
G3	1	$[2, 5.5]$

Table 1 Parameters of the different type of gamma instances.

windows are the only difference between the instances in a Solomon set, there is one instance per Solomon set, i.e., c1, c2, r1, r2, rc1, rc2. The service times of the customers are adjusted based on the modification in the planning horizon, i.e., if the planning horizon increases with factor x then the service time increases with factor x as well. The vehicle capacity and the location and demand of the customers remain the same as in the original Solomon instances. If instances with N customers are considered, then the first N customers of the original 100 customers are taken into account.

7.1.2. Arc selection measures

Because using a complete graph in the solution method unnecessarily leads to high computation times, we must find a way to reduce the number of arcs while maintaining high quality solutions. Since the risk of violating the assigned time windows is being minimized, it is unlikely that arcs with a wide travel time distribution are used in the optimal solution. Furthermore, the expected travel time cannot increase too much compared to the minimum expected travel time of the CRVP. Therefore, arcs with high mean travel time and wide distribution are unlikely to be used in the optimal solution. Let c_a be the mean travel time of arc a and let $\Delta_a = \overline{c}_a - \underline{c}_a$ be the difference between the maximum and minimum value of the travel time of arc a. To reduce the number of arcs, an arc measures is used to rank the arcs. Let $a = (i, j)$ be an arc, then the measure is given by $c_a / \mathbb{E}_{b \in \delta^-(j)} c_b + \Delta_a / \mathbb{E}_{b \in \delta^-(j)} \Delta_b$. The mean travel time of arc (i, j) is divided by the average mean travel time of the incoming arcs of node j, to measure the performance of the arc relative to the other incoming arcs of node j. The same holds for the difference parameter Δ_a. To reduce the number of arcs, the best three incoming arcs and the best three outgoing arcs are selected for every node. The performance of this arc selection measure compared to other measures is tested in Appendix C. The new instances generated by this measure have on average $5.7N$ edges in total. The characteristics of the instances are given in Appendix D. The average mean arc length decreases from G1 to G3 and from T1 to T3. Furthermore, the average difference between the maximum and minimum travel time, denoted by Δ, fluctuates with less than 1% between G1, G2, and G3 and between T1, T2, and T3.

7.2. Performance of the branch-and-cut algorithm

In this section, the performance of branch-and-cut algorithm for the RVRP-TWA is tested. The objective is to find the routing solution with the lowest time window violation index while the

expected travel time is below a certain threshold value. This threshold value is set to $1.05T_0$, with T_0 the minimum expected travel time of the VRP. For the VRP-based solution, the time windows are assigned such that the time window violation index is minimized, i.e., the method in Section 4.2 is used to determine τ_i for all $i \in \mathcal{N}_T$ in the final routing solution. Hence, it is a two-step procedure of route first and TWA second.

The average results of the triangular and gamma instances are presented in Tables 2 and 3, respectively. The number of customers in the instances is denoted in the first column. The number of instances solved out of 6 instances is reported in column "nS". The average number of vehicle used is reported in the column "nV" and the average computational time in seconds is reported in the column "time". The average upper bound of the time window violation index is presented in column "risk" and the average number of subgradient cuts added to the formulation is presented in the column "nC". In columns "Δrisk" and "Δtt", the relative difference of the violation index and the travel time compared to the VRP-based solution are given. The difference is computed by $(R - R_0)/R_0$, with R_0 denoting the violation index corresponding to the VRP-based solution and R the violation index of the RVRP-TWA solution. A similar calculation is performed for the difference in travel time. If an instance is not solved within two hours and the upper bound of time window violation index is equal to zero, then no feasible solution is found and this solution is not taken into account when calculating the average values. The detailed results per instance can be found in Appendix E.

	T1							T2							T3						
N	nS	nV	time	risk	nC	Δrisk	Δtt	nS	nV	time	risk	nC	Δrisk	Δtt	nS	nV	time	risk	nC	Δrisk	Δtt
10	6	1.2	0	36	6	-13%	3%	6	1.2	1	55	13	-38%	3%	6	1.2	1	74	7	-25%	3%
15	6	1.5	8	37	15	-57%	3%	6	1.5	17	52	20	-40%	3%	6	1.5	6	68	14	-44%	4%
20	6	1.7	22	104	17	-21%	3%	6	1.7	79	81	32	-47%	3%	6	1.7	31	134	17	-34%	4%
25	6	2.3	1001	73	46	-52%	4%	6	2.0	405	176	36	-40%	3%	6	2.0	491	86	76	-31%	4%
30	2	2.5	4921	107	32	-49%	4%	4	2.5	3993	131	77	-34%	4%	3	2.5	5108	185	79	-49%	4%
35	0	2.8	7200	128	64	-35%	5%	1	2.8	6608	132	44	-28%	4%	1	2.8	6171	99	68	-38%	4%

Table 2 Average results of the triangular instances.

For the triangular instances, the time window violation index of both the VRP-based and the RVRP-TWA solutions increase on average from T1 to T3. Hence, instances with skewed travel times have a higher risk, since the magnitude of the violations increases. The difference in risk value between the robust solution and the VRP-based solution is, on average, 39% while the travel time increases with only 3.6% on average. In Figure 1, the routing solution of the VRP and RVRP-TWA are presented for the T3-r2 instance with 10 customers. It should be noted that for different values

	G1							G2							G3						
N	nS	nV	time	risk	nC	Δrisk	Δtt	nS	nV	time	risk	nC	Δrisk	Δtt	nS	nV	time	risk	nC	Δrisk	Δtt
10	6	1.2	3	133	37	-19%	4%	6	1.2	2	125	28	-19%	4%	6	1.2	2	95	17	-26%	3%
15	6	1.5	65	233	71	-24%	4%	6	1.5	35	222	64	-23%	4%	6	1.5	24	176	29	-28%	4%
20	6	2.0	1970	363	162	-26%	4%	6	2.0	1001	352	106	-21%	5%	6	1.8	197	289	40	-31%	5%
25	3	2.3	4661	450	159	-20%	4%	4	2.3	4842	394	189	-34%	4%	6	2.0	2558	446	129	-26%	3%
30	0	2.8	7200	539	109	-26%	4%	1	2.7	6833	711	102	-20%	5%	1	2.7	6246	373	84	-26%	5%

Table 3 Average results of the gamma instances.

of N, the time window violation index of instance c1 is already zero for the VRP-based solution. Therefore, in this case, the RVRP-TWA will not improve the risk value.

For the gamma instances, the time window violation index of both the RVRP-TWA and the VRP-based solutions decrease from G1 to G3. This is because the standard deviation of the difference between the maximum and minimum travel time increases from G1 to G3 while the average difference stays the same (see Appendix D). Therefore, for the G3 instances, there are more arcs with low variability which results in lower risk values. The computational time also decreases from G1 to G3. The average difference in risk value compared to the VRP-based solution is 25% while the travel time increases with on average 4.2%. The solutions of the G3 instances result in the highest reduction in time window violation index compared to the VRP-based solutions.

For both the triangular and gamma instances, the set 2 Solomon instances have a higher time window violation index than the set 1 instances. This is due to the larger vehicle capacity and shorter service times of the set 2 instances (see Section 7.1.1 for the description of these adjusted Solomon instances). As a result, less vehicles are used and more customers are included in a single route resulting in more uncertainty than in the set 1 instances. Furthermore, for instances with $N \leq 20$ customers, the set 2 Solomon instances are easier to solve than the set 1 instances, since the set 2 Solomon instances only need a single vehicle. The branch-and-cut algorithm solves all triangular instances with 25 customers or less to optimality and all gamma instances with 20 customers or less. For the instances with 30 customers, the algorithm solves 9 triangular instances but only 2 gamma instances. The triangular instances are easier to solve because the standard deviation of the mean travel time and the standard deviation of the difference between the maximum and minimum travel time are both much higher in the triangular instances than in the gamma instances (see Appendix D). If the standard deviation of the mean travel time is larger, many arcs cannot be used in the optimal solution due to the constraint on the total expected travel time, which makes the instances easier to solve. Furthermore, the high standard deviation of the difference between the maximum and minimum travel times indicates that there are arcs with very low variability, which results in a low risk value. Therefore, the time window violation indexes of the triangular instances are lower than of the gamma instances.

Overall, the computational time of the branch-and-cut algorithm is higher when more cuts are generated. The number of cuts represents the number of feasible solutions found by the algorithm. The computational time of the branch-and-cut algorithm significantly increases when the number of customers increases. The computational times of instances with 20 customers is on average 69 and 419 times higher than the instances with 10 customers, for the triangular and gamma instances, respectively. Note that if an instance is not solved, the lower bound is relatively low.

7.3. Evaluation optimal time window assignment method

In the proposed solution framework, a time window assignment method is used to minimize the time window violation index for a given route, as described in Section 4.2. In this section, the performance of this time window assignment method is compared with other time window assignments policies. Similar as in Vareias, Repoussis, and Tarantilis (2017), three different policies for τ_i are evaluated: τ_i is selected symmetrically around the average arrival time, i.e., $\tau_i = \mathbf{cs}^i - \epsilon_i/2$; τ_i is skewed left with respect to the average arrival time, i.e. $\tau_i = \mathbf{cs}^i - \epsilon_i$; and τ_i is skewed right with respect to the average arrival time, $\tau_i = \mathbf{cs}^i$. In these policies, the value of τ_i is fixed given the average arrival time at customer i. These policies can also be used in our solution framework. The definition of $f(\mathbf{s})$ and the subgradient of $f(\mathbf{s})$ for these three policies are described in Appendix F.

The average results of the four time window assignment policies on the instances with 10, 15, 20 and 25 customers are presented in Table 4. The results of the algorithm with the minimum time window violation index policy, described in Section 4.2, is presented in column "min". The results of the algorithm with τ_i determined by the symmetric, left skewed and right skewed policy around the average arrival time are presented in the columns "sym", "left", and "right", respectively. For every time window assignment policy, the average time window violation index and the expected travel time of the final routing solution are reported in columns "risk" and "tt", respectively. The average time window violation as defined in Section 6 is calculated using a simulation with 100,000 scenarios. This average violation and the corresponding standard deviation are given in columns "V" and "sdV", respectively.

Our proposed policy and the symmetric policy perform significantly better than the skewed left and right policies. Since the travel time distributions are right-skewed, the probability of arriving earlier than the mean value is higher, therefore, the left skewed policy performs better than the right skewed policy. Our proposed policy has the lowest time window violation index. However, according to the simulation results, the symmetric policy performs slightly better in terms of average violation than our proposed policy. This is because the total travel time distribution is a sum of the travel time distribution of all arcs and by the law of large numbers the total distribution is flatter and more symmetric around the mean value than the original travel time distributions.

	min				sym				left				right			
Inst	risk	tt	V	sdV	risk	tt	V	sdV	risk	tt	V	sdV	risk	tt	V	sdV
T1	62.2	278.7	0.18	1.0	62.4	278.8	0.18	0.9	437.0	278.5	8.02	12.0	484.7	279.3	8.92	12.2
T2	91.1	266.3	0.66	2.3	91.2	266.2	0.66	2.3	557.0	267.0	9.89	15.3	709.0	266.6	12.69	16.9
T3	90.7	253.5	1.20	4.6	91.1	253.1	1.21	4.7	499.7	252.2	10.88	18.3	890.1	252.9	19.06	24.8
avg	81.4	266.2	0.68	2.6	81.6	266.0	0.68	2.6	497.9	265.9	9.59	15.2	694.6	266.3	13.56	18.0
G1	296.7	316.3	4.96	13.5	297.2	316.3	4.94	13.4	2123.8	316.5	31.01	43.2	2379.2	315.6	34.60	41.7
G2	239.9	275.7	4.80	13.9	240.7	275.7	4.71	13.7	1525.2	274.7	25.65	38.3	2015.0	275.2	33.66	37.7
G3	252.1	273.3	8.13	21.8	253.2	273.3	7.88	21.3	1406.9	272.6	25.33	42.7	2171.7	271.8	41.56	42.2
avg	262.9	288.4	5.96	16.4	263.7	288.4	5.84	16.1	1685.3	287.9	27.33	41.4	2188.6	287.5	36.60	40.5

Table 4 Average results for the different time window assignment policies.

Since the aim of the robust approach is to seek a robust solution which minimizes the worst case distributions (shown in the column "risk"), the robust solution may not necessarily be the best in terms of the average violation under a given distribution. However, one can see that the differences in the expected violations between the robust solution "min" and the symmetric case "sym" are very small. It should be noted that the difference in the average violation of the minimum and symmetric policy increases when the travel time distributions are more skewed (from T1 to T3 and G1 to G3).

In reality, some arcs are less sensitive to disruptions than others. Therefore, the instances were adjusted by assuming that 50% of the arcs in the arc set have a uniform travel time of length two around the mean travel time. The new instances are denoted by a prime symbol. The results of the minimum and symmetric time window assignment policies on these new instances are presented in Table 5. Due to the reduction of the variability of the travel times, the average time window violation index and average time window violation are lower for these new instances. Table 5 shows that the proposed minimum policy performs better than the symmetric policy in terms of violation index, average violation and standard deviation. The difference in risk between these two policies increases when the travel time distributions are more skewed. The lower standard deviation indicates that the proposed solution is more robust than the symmetric method. Based on these experiments, we conjecture that the difference between the minimum and symmetric policy increases when less arcs are sensitive to disruptions.

7.4. Comparison with other models

In this section, the proposed RVRP-TWA is compared with the SVRP-TWA and the VRP-based approach. The VRP-based approach is a two-step process of route first and TWA second, i.e., first, the routes are determined by minimizing the expected travel time, and secondly, the time windows are assigned for the final routing solution. In the VRP-based approach the travel time uncertainty is ignored when constructing the route and the time windows are assigned such that the time window violation index is minimized, i.e., using the method described in Section 4.2. This

	min				sym			
Inst	risk	tt	V	sdV	risk	tt	V	sdV
T1′	26.4	284.0	0.06	0.4	26.4	284.6	0.05	0.4
T2′	14.8	273.7	0.01	0.1	14.9	273.3	0.01	0.2
T3′	39.2	264.7	0.29	1.8	39.8	264.6	0.36	2.1
avg	26.8	274.1	0.12	0.8	27.0	274.2	0.14	0.9
G1′	101.7	334.5	1.27	4.7	102.1	334.7	1.31	4.7
G2′	60.6	295.8	0.72	3.9	61.3	295.8	0.75	4.2
G3′	50.0	299.9	0.85	6.0	51.1	299.8	0.98	6.6
avg	70.8	310.0	0.95	4.9	71.5	310.1	1.01	5.2

Table 5 Average results for the minimum and symmetric time window assignment policy.

model will be compared to the proposed RVRP-TWA that takes characteristics of the travel time distributions into account.

The proposed SVRP-TWA assumes that the travel time distributions are known and the expected time window violation is minimized. The proposed algorithm for the SVRP-TWA is described in Section 6 and the sampling method with 100,000 scenarios is used in this experiment. Even though the stochastic and robust VRP-TWA models are developed for different purposes in which different assumptions and objectives are taken into account, the computational comparisons in this section provide interesting insights between the two approaches on different aspects.

The solutions of the three models are tested in a simulation to calculate the average time window violation, i.e., the average number of minutes that a vehicle arrives too early or too late at all customers in the solution. To evaluate the robustness of the solutions, two different travel time distributions with the same characteristics are used. The first distribution is the triangular (or gamma) distribution of the original instances described in Section 7.1. As second distribution, a mixture of two triangular distribution is used (denoted by MT distribution) which has the same mean, minimum, and maximum values as the original instance. This MT distribution has two modes which are different from the mode of the original function. Appendix G describes how these MT distributions are generated from the original distributions. For the VRP-based and the robust approach, the final solution will be the same for both distributions. For the stochastic approach the distribution does matter. Therefore, two different travel time distributions of the SVRP-TWA are tested: one in which the original distribution is assumed (Stoch-T or Stoch-G) and one in which the new MT distribution is assumed (Stoch-MT). When the same scenarios are used in the SVRP-TWA as in the simulation, the SVRP-TWA gives the optimal solution when minimizing the average time window violation. This is not the case when the distribution used in the optimization model of the SVRP-TWA is different from the distribution used in the simulation.

The average results for each model are reported in Table 6 and 7 for the instances with 10, 15, 20, and 25 customers. The results of the instances that were solved by all models are reported. The distribution used in the simulation is reported in the first column, the number of instances solved by all models is reported in the second column, and the model is given in the third column. For each method, the average computational time in seconds and the average time window violation index are presented in the columns "time" and "risk", respectively. The other columns present the result from the simulation, with in column "avTT" and "sdTT" the average and standard deviation of the total travel time, respectively. The average number of minutes that all vehicles in a solution are too early, too late and in total outside the time windows are reported in the columns "lbV", "ubV" and "V", respectively. The standard deviation of the total violation is reported in "sdV" and the maximum violation over all scenarios in "maxV". In the last two columns, the number of scenarios with no time window violations and five or more violations are reported.

												#V(×1000)	
distr	solved	model	time	risk	avTT	sdTT	lbV	ubV	V	sdV	maxV	0	≥ 5
T	71/72	VRP	14	126.2	**254.5**	**16.3**	0.5	1.0	1.5	5.0	101.2	89.8	3.0
		Robust	138	**80.8**	263.4	16.5	0.2	0.5	0.7	2.6	64.8	93.4	**1.4**
		Stoch-T	198	85.5	263.1	16.5	0.2	0.4	**0.6**	**2.4**	**62.9**	**93.9**	**1.4**
T-MT	70/72	VRP	13	126.7	**254.3**	**16.7**	38.1	42.7	80.8	40.9	247.2	29.8	55.8
		Robust	115	**81.4**	263.1	16.9	27.5	30.6	58.1	**29.4**	**183.4**	35.2	47.4
		Stoch-MT	184	99.4	263.4	16.9	23.0	33.4	**56.4**	31.4	188.2	**35.8**	**47.2**
G	59/72	VRP	4	338.2	**278.5**	**17.4**	2.9	6.3	9.2	23.3	419.7	65.5	12.6
		Robust	374	**260.2**	289.8	17.6	1.7	4.3	6.0	16.7	328.7	**71.9**	8.8
		Stoch-G	242	267.8	289.8	17.6	2.0	3.6	**5.6**	**15.0**	**308.9**	71.5	**8.7**
G-MT	58/72	VRP	4	332.8	**274.7**	**18.0**	69.0	76.6	145.6	84.6	571.3	4.3	80.3
		Robust	351	**256.1**	285.8	18.2	52.5	59.7	112.2	**67.7**	**469.1**	**5.7**	**73.7**
		Stoch-MT	200	288.3	285.7	18.2	46.7	63.5	**110.2**	70.5	475.8	5.6	75.2

Table 6 Results for the VRP-based, RVRP-TWA, and SVRP-TWA with the same distribution in the SVRP-TWA as in the simulation.

In Table 6, the distributions used in the stochastic model and in the simulation are the same. As expected, the average total travel time is lowest for the VRP-based approach and the robust solution has the lowest time window violation index. The standard deviation of the total travel time is also lowest for the VRP-based approach. The travel time of the RVRP-TWA can increase with maximum 5% compared to the VRP-based solution, however, the results show that the increase in travel time is less than 4% on average. The average decrease in time window violation index when using the RVRP-TWA instead of the VRP-based solution is 30% and the decrease in average violation is even higher (36%). The standard deviation and maximum violations are lower for the

RVRP-TWA. Furthermore, for the solution of the RVRP-TWA, there are more scenarios without violations and the number of scenarios with 5 violations or more is lower for the RVRP-TWA than for the VRP-based approach. Hence, for a relatively small increase in travel time (4%), the accuracy of being on time increases a lot when using the RVRP-TWA instead of the VRP-based approach.

The stochastic model gives the optimal solution when minimizing the average violation. The RVRP-TWA increases with on average 6% compared to the optimal SVRP-TWA. However, the number of scenarios without violations or with five violations or more are similar for both models. Furthermore, for the MT distribution, the standard deviation of the violation and the maximum violation are lower for the robust model. The average and standard deviation of the travel time are almost the same for the robust and stochastic model. Thus, while the robust method has less data requirements than the stochastic variant it performs very well.

												#V(×1000)	
distr	solved	model	time	risk	avTT	sdTT	lbV	ubV	V	sdV	maxV	0	≥ 5
T	70/72	Robust	115	**81.4**	**263.0**	16.5	0.2	0.5	**0.7**	**2.6**	**65.6**	**93.3**	**1.4**
		Stoch-MT	184	99.4	263.3	16.5	0.2	0.8	1.0	3.3	73.0	91.2	1.8
T-MT	71/72	Robust	138	**80.8**	263.4	**16.9**	27.2	30.4	**57.6**	**29.2**	**182.9**	**34.9**	**47.7**
		Stoch-T	198	85.5	**263.2**	17.0	30.7	29.1	59.8	30.1	183.1	32.4	49.2
G	58/72	Robust	351	**256.1**	**285.9**	17.5	1.7	4.3	**6.0**	**16.7**	**329.6**	**72.2**	**8.7**
		Stoch-MT	245	288.3	286.1	17.5	1.1	6.1	7.2	18.8	340.5	69.5	9.4
G-MT	59/72	Robust	374	**260.2**	**289.7**	18.3	52.0	59.2	**111.2**	67.6	471.5	5.8	**73.4**
		Stoch-G	242	267.8	**289.7**	18.3	58.9	53.8	112.7	**65.8**	**449.2**	**6.4**	74.7

Table 7 Results for the RVRP-TWA and SVRP-TWA with different distribution in stochastic model and in the simulation.

In Table 7, the distribution assumed in the stochastic model and the distribution used in the simulation are different. Since the characteristic of both distributions are the same, the solutions of the VRP-based and the robust model stay the same as in Table 6. Therefore the VRP-based results are excluded from this table. Table 7 compares the performance of the stochastic and robust approaches when no accurate estimate could be made on the actual travel time distributions. The results show that the robust model performs significantly better than the stochastic model. The average violation of the RVRP-TWA is on average 14% lower than of the SVRP-TWA model and the number of scenarios with 5 violations or more is lower for the RVRP-TWA. Furthermore, in most cases, the standard deviation and the maximum violation of the robust model are also lower than that of the stochastic model. Hence, the robust solution method is much less sensitive to distributional uncertainty than the stochastic solution approach.

Overall, the simulation with the MT distribution leads to higher violations and more violations per scenario. This is because the modes in the MT distribution are further away from the mean travel time. It should be noted that if the time window violation index decreases a lot, then the average time window violation decreases as well. If the differences in time window violation index are small, then a higher index value does not imply a higher average time window violation. Thus, the time window violation index is a good measure for the average time window violation when the difference between solutions is not too small.

7.5. Pareto frontier

In the RVRP-TWA, the time window violation index is minimized while the expected travel time must be below ρT_0. Until now it has been assumed that $\rho = 1.05$, hence the expected travel time could increase with maximum 5% compared to the minimum expected travel time of the VRP. Furthermore, the time window length was set to $\epsilon_i = \hat{\epsilon} = 30 \; \forall i \in \mathcal{N}_T$, where $\hat{\epsilon}$ is a predefined window length. In this section, we will investigate the sensitivity of the proposed branch-and-cut algorithm to these two parameters and we show the trade-off between travel time and the risk value.

In Table 8, the average time window violation index and computational times are given for different values of $\hat{\epsilon}$ for the triangular "T" and gamma "G" instances. The second column represents the number of customers taken into account and the number of instances solved is reported in column "solved". An instance is only taken into account if it is solved for all $\hat{\epsilon}$ values. Trivially, the time window violation index decreases when the time window length increases. For the triangular instances, the time window violation index decreases with on average 62% from $\hat{\epsilon} = 15$ to $\hat{\epsilon} = 30$ and with 50% from $\hat{\epsilon} = 30$ to $\hat{\epsilon} = 45$. For the gamma instances, this decrease is 54% and 41%. Hence, the decrease in time window violation index is not linear. The incremental decrease in risk value declines when the number of customers increases. For instance T2-r1, the Pareto frontier for different time window lengths and travel time threshold values is presented in Figure 3. For this instance is shown that the risk gap between a time window length of 15 and 30 minutes is much larger than the gap between 30 and 45 minutes. Since the travel time threshold is set to $\rho = 1.05$ the average travel time stays the same for all ϵ values.

The influence of the travel time threshold parameter ρ is presented in Table 9. When the threshold increases, the solution space of the feasible routing solutions increases and therefore the computational time increases. On average, the computational time increases faster when more customers are taken into account in the instances. Due to this increase in solution space, the time window violation index decreases. This decrease in violation index is, on average, 14% from $\rho = 1$ to $\rho = 1.025$ and 16% from $\rho = 1.025$ to $\rho = 1.05$. For larger threshold values this incremental decrease in the time window violation index declines. The example in Figure 3 illustrates the steep decrease in the

			$\hat{\epsilon}=15$		$\hat{\epsilon}=30$		$\hat{\epsilon}=45$	
Inst	N	solved	time	risk	time	risk	time	risk
T	10	18/18	0.7	156.4	0.6	54.8	0.5	24.2
	15	18/18	10.9	153.2	10.4	52.2	6.5	22.6
	20	18/18	57.1	277.2	44.2	106.6	34.6	53.3
	25	18/18	699.0	268.5	632.1	111.7	1092.4	64.0
	average		191.9	213.8	171.8	81.3	283.5	41.0
G	10	18/18	2.1	271.8	2.3	117.9	2.3	64.7
	15	18/18	33.1	473.7	41.3	210.5	40.7	119.9
	20	15/18	167.3	777.9	182.7	360.0	186.7	215.9
	25	12	2492.5	972.8	2574.3	456.7	2833.9	276.5
	average		524.6	583.5	546.3	266.5	596.5	156.8

Table 8 **Average time window violation index and computational time for different time window lengths.**

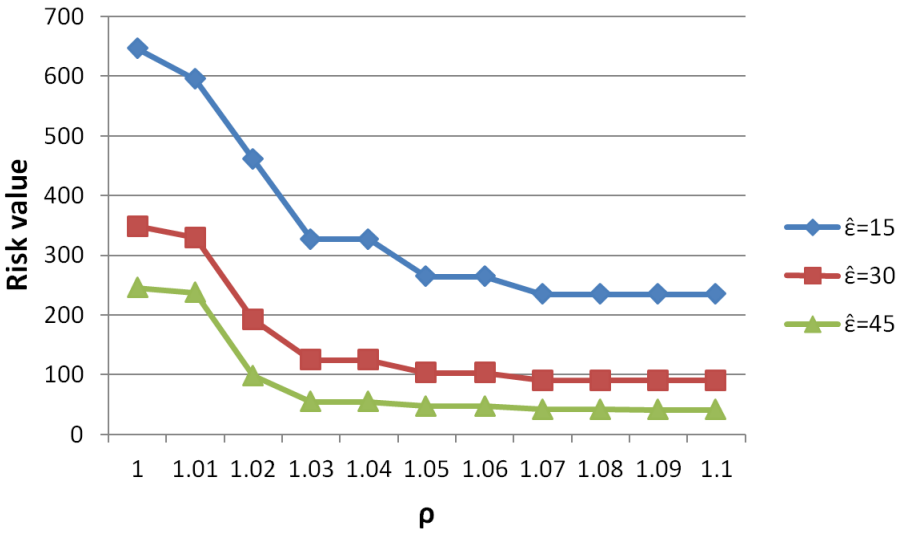

Figure 3 **Pareto frontier for instance T2-r1 with 20 customers.**

time window violation index when ρ is increased from 1.01 to 1.03 and that this decrease tapers off when ρ increases. The frontier is S-shaped because ρ should increase enough such that there exists a new routing solution with a lower violation index and when the optimal routing solution is found increasing ρ does not help anymore. In column "Δtt" the difference between the average travel time compared to the VRP based solution ($\rho=0$) is shown. When the average travel time threshold is set to $\rho=1.05$ an increase of 5% of the travel time is allowed. However, the travel time of the final solution increases with on average 3.4% for a triangle instance and with 4.2% for a gamma instance.

From a managerial point of view the risk of violating a time window can be significantly reduced by allowing the travel time to increase with only 2.5% to 5%. Furthermore, the time window length can be chosen corresponding to the preferred risk certainty.

			$\rho = 1$		$\rho = 1.025$			$\rho = 1.05$			$\rho = 1.075$			$\rho = 1.1$		
Inst	N	solved	time	risk	time	risk	Δtt	time	risk	Δtt	time	risk	Δtt	time	risk	Δtt
T	10	18/18	0	81	0	70	0.6%	1	55	3.1%	1	41	5.4%	1	39	6.2%
	15	18/18	2	92	3	71	1.4%	9	52	3.6%	22	49	4.8%	42	48	6.4%
	20	18/18	3	176	15	137	1.4%	51	107	3.4%	110	102	5.4%	259	99	6.8%
	25	12/18	7	150	50	133	1.6%	238	128	3.3%	567	126	5.1%	1695	125	6.8%
	average		3	122	14	100	1.3%	60	81	3.4%	140	75	5.2%	391	73	6.6%
G	10	18/18	0	147	1	131	1.0%	2	118	3.9%	5	109	5.2%	10	106	7.7%
	15	18/18	1	275	8	235	1.8%	40	210	4.1%	171	193	6.3%	643	184	8.7%
	20	14/18	8	469	28	428	1.8%	177	343	4.4%	1150	316	6.6%	1573	301	8.7%
	average		3	283	11	251	1.6%	65	214	4.2%	385	198	6.1%	675	189	8.4%

Table 9 Average time window violation index and computational time for different threshold values.

8. Conclusions and future research

In the VRP-TWA, the time window assignment problem and the vehicle routing problem are combined. Recent papers propose heuristic solution methods to solve the stochastic VRP-TWA in which the probability distributions of the travel times are known. We are the first to formulate the robust VRP-TWA to handle cases in which the probability distributions are hard to estimate. In the RVRP-TWA, it is assumed that the distribution of the travel times are uncertain and only some descriptive statistics are available. The risk of violating the assigned time windows is minimized, while ensuring that the expected travel time is lower than a certain threshold value. To measure the risk of violating the assigned time windows, the time window violation index based on the requirements violation index proposed by Jaillet, Qi, and Sim (2016) is used. An exact method is proposed to solve the subproblem of assigning a time window to each customers in a given route with minimum time window violation index. We show that this subproblem is convex and that the subgradient cuts can be generated. These cuts are used in a branch-and-cut framework to exactly solve the RVRP-TWA. The experiments show that the branch-and-cut algorithm is able to solve instances up to 35 customers. Furthermore, the trade-off between the expected total travel time and the time window violation index is shown. Allowing the travel time to increase with maximum 5% compared to the minimum travel time, decreases the time window violations by, on average, 33%.

The solution quality and robustness of the RVRP-TWA model is tested by comparing it to a stochastic variant of the VRP-TWA in which the travel time distributions are known. An exact solution method is proposed for the SVRP-TWA using a branch-and-cut framework. Using the SVRP-TWA model, we have shown that the robust solution is close to the optimal solution. Furthermore, when the travel time distributions are uncertain the robust approach performs better than the stochastic approach.

To solve larger instances, the subproblem of minimizing the time window violation index for a given routing solution could be incorporated in a heuristic framework. Furthermore, the variant of the VRP-TWA with hard time windows, in which the vehicle has to wait when it arrives before the time window, could be an interesting topic for future research. Hard time windows are more difficult to solve exactly, since the arrival time cannot be calculated by the sum of the independent travel times of the arcs. However, the stochastic variant can be solved with the sampling based approach proposed in this chapter. It would also be interesting to develop new risk measures for the robust approach that take other characteristics of the travel time distribution into account.

Extensions: variable time window length and correlated travel times

In this section, two extensions of the proposed method are discussed; time window length as a decision variable and correlated travel times.

Variable time window length

We assumed that the length of a time window per customer is an input variable that can be chosen by the decision maker. Our approach can be extended to the case where ϵ_i is a decision variable with linear cost. The problem would become even more complex since the solution space will increase for a given route. However, the same proposed methodology and solution method can be used. Due to the extra decision variable, an extra KKT condition must be added and therefore the subgradient will be slightly adjusted.

Correlated travel times

In practice, the travel times of arcs may be correlated. However, most papers on travel time uncertainty assume independent travel times to avoid a tremendous increase in model complexity or data availability. Jaillet, Qi, and Sim (2016) propose a way to include correlation without increasing the complexity of the algorithm too much. We briefly describe how this approach can be applied in our setting.

As suggested in the paper of Jaillet, Qi, and Sim (2016), the travel times can be expressed as a linear function of independent factors, i.e.,

$$\tilde{z}_a = z_a^0 + \sum_{j=1}^{B} z_a^j \tilde{c}_j, \quad \forall a \in \mathcal{A}$$

Where $\tilde{c}_1, \ldots, \tilde{c}_B$ are independent distributed factors which represent for example the weather conditions, occurence of traffic jams, etc. The coefficient of these factors can be estimated by a linear regression. Note that this method can only be used when a lot of data is available to first

create the distribution of these factors and second estimate the coeffients by regression. When the formula for $\tilde{z}_a$ is estimated then this can incorporated as follows

$$C_{\alpha_i}(\tilde{t}_i) = C_{\alpha_i}(\tilde{\mathbf{z}}\mathbf{s}^i) = C_{\alpha_i}\left(\sum_{a\in\mathcal{A}}(z_a^0 + \sum_{j=1}^{B} z_a^j \tilde{c}_j)s_a^i\right) = C_{\alpha_i}\left(\mathbf{z}^{0^T}\mathbf{s}^i + \sum_{j=1}^{B}\tilde{c}_j\mathbf{z}^{j^T}\mathbf{s}^i\right) = \mathbf{z}^0\mathbf{s}^i + \sum_{j=1}^{B} C_{\alpha_i}(\tilde{c}_j\mathbf{z}^{j^T}\mathbf{s}^i)$$

When using this function in the problem formulation, the calculation of the function $C_{\alpha_i}(\tilde{\mathbf{z}}\mathbf{s}^i)$, $C_{\eta_i}(-\tilde{\mathbf{z}}\mathbf{s}^i)$ and its subgradients will change. The subgradients can be calculated in a relatively straightforward manner and the proposed methodology in this paper can be applied directly.

Acknowledgments

This research was enabled, in part, by support provided by Compute Canada (www.computecanada.ca) and by The Netherlands Organisation for Scientific Research (NWO) under grant 407-13-050. This support is gratefully acknowledged.

Appendix A: Properties of the time window violation index

The risk of violating the endogenous time window $[\tau_i, \tau_i + \epsilon_i]$ at node i is measured by the time window violation index defined by

$$\rho_{\tau_i} = \inf\{\alpha_i + \eta_i | C_{\alpha_i}(\tilde{t}_i) \le \tau_i + \epsilon_i, C_{\eta_i}(-\tilde{t}_i) \le -\tau_i\}.$$

Let $C_{\alpha_i}(\tilde{t}_i)$ be the deterministic value representing the worst case certainty equivalent of random arrival time $\tilde{t}_i$ at node i under risk tolerance parameter α_i. $C_{\alpha_i}(\tilde{t}_i)$ is defined as:

$$C_{\alpha_i}(\tilde{t}_i) = \begin{cases} \sup_{\mathbb{P}\in\mathbb{F}} \alpha_i \ln \mathbb{E}_{\mathbb{P}}\left(\exp\left(\frac{\tilde{t}_i}{\alpha_i}\right)\right) & \text{if } \alpha_i > 0 \\ \lim_{\beta\downarrow 0} C_\beta(\tilde{t}_i) & \text{if } \alpha_i = 0. \end{cases}$$

Jaillet, Qi, and Sim (2016) showed the time window violation index has the following useful properties:

- The certainty equivalent $C_{\alpha_i}(\tilde{t}_i)$ decreases when the risk tolerance parameter α_i increases, i.e., $C_{\alpha_i}(\tilde{t}_i)$ is decreasing in α_i and strictly decreasing when $\tilde{t}_i$ is not a constant. Therefore, the time window violation index increases when the risk of violating the time window increases, i.e.

$$\lim_{\alpha_i\downarrow 0} C_{\alpha_i}(\tilde{t}_i) = \bar{t}_i = \bar{\mathbf{c}}\mathbf{s}^{\mathbf{i}}, \quad \lim_{\alpha_i\to\infty} C_{\alpha_i}(\tilde{t}_i) = \mathbb{E}(\tilde{t}_i).$$

- The time window violation index is zero only if the arrival time is guaranteed to meet the time window, i.e., $\rho_{\tau_i} = 0$ if and only if $\mathbb{P}(\tilde{t}_i \in [\tau_i, \tau_i + \epsilon_i] = 1)$ for all $\mathbb{P} \in \mathbb{F}$.

- If the expected arrival time lies outside the assigned time window, then the time window violation index is infinite, i.e., if $\sup_{\mathbb{P}\in\mathbb{F}} \mathbb{E}_{\mathbb{P}}(\tilde{t}_i) \notin [\tau_i, \tau_i + \epsilon_i]$ or $\inf_{\mathbb{P}\in\mathbb{F}} \mathbb{E}_{\mathbb{P}}(\tilde{t}_i) \notin [\tau_i, \tau_i + \epsilon_i]$ then $\rho_{\tau_i} = \infty$. In this case, the assigned time window is not feasible.

- The time window violation index specifies bounds on the probability of violations for every magnitude of violation, i.e., if $\rho_{\tau_i} \ge 0$ then $\forall \mathbb{P} \in \mathbb{F}$ and $\forall \theta > 0$

$$\max\{\mathbb{P}(\tilde{t}_i < \tau_i - \theta), \mathbb{P}(\tilde{t}_i > \tau_i + \epsilon_i + \theta)\} \le \exp(-\theta/\rho_{\tau_i}).$$

  Because of this property both the probability and the magnitude of violations are taken into account in the time window violation index.

- $C_{\alpha_i}(\tilde{t}_i)$ is jointly convex in $(\alpha_i, \tilde{t}_i)$.
- The certainty equivalent $C_{\alpha_i}(\tilde{t}_i)$ is additive for independent random variables, i.e., if random variables $\tilde{t}_1$ and $\tilde{t}_2$ are independent of each other, then for any $\alpha_i \geq 0$, $C_{\alpha_i}(\tilde{t}_1 + \tilde{t}_2) = C_{\alpha_i}(\tilde{t}_1) + C_{\alpha_i}(\tilde{t}_2)$.

Because of this last additivity property, we have $C_{\alpha_i}(\tilde{t}_i) = C_{\alpha_i}(\tilde{\mathbf{c}}\mathbf{s}^{\mathbf{i}}) = \sum_{a\in\mathcal{A}} C_{\alpha_i}(\tilde{c}_a s_a^i)$. For the distributions in which the mean, minimum, and maximum travel time are known the equations of $C_{\alpha_i}(\tilde{c}_a s_a^i)$ and $C_{\eta_i}(\tilde{c}_a s_a^i)$ are obtained in Jaillet, Qi, and Sim (2016) and Adulyasak and Jaillet (2016). These equations are given by

$$
\begin{aligned}
C_{\alpha_i}(\tilde{c}_a s_a^i) &= \sup_{\mathbb{P}\in\mathbb{F}} \alpha_i \ln \mathbb{E}_{\mathbb{P}}\left(\exp\left(\frac{\tilde{c}_a s_a^i}{\alpha_i}\right)\right) \\
&= \begin{cases} \alpha_i \ln\left(\frac{(\overline{c}_a-\mu_a)\exp(\frac{\underline{c}_a s_a^i}{\alpha_i})+(\mu_a-\underline{c}_a)\exp(\frac{\overline{c}_a s_a^i}{\alpha_i})}{\overline{c}_a-\underline{c}_a}\right) & \text{if } \alpha_i > 0 \\ \overline{c}_a & \text{if } \alpha_i = 0 \end{cases} \\
C_{\eta_i}(-\tilde{c}_a s_a^i) &= \sup_{\mathbb{P}\in\mathbb{F}} \eta_i \ln \mathbb{E}_{\mathbb{P}}\left(\exp\left(-\frac{\tilde{c}_a s_a^i}{\eta_i}\right)\right) \\
&= \begin{cases} \eta_i \ln\left(\frac{(\overline{c}_a-\mu_a)\exp(-\frac{\underline{c}_a s_a^i}{\eta_i})+(\mu_a-\underline{c}_a)\exp(-\frac{\overline{c}_a s_a^i}{\eta_i})}{\overline{c}_a-\underline{c}_a}\right) & \text{if } \eta_i > 0 \\ -\underline{c}_a & \text{if } \eta_i = 0 \end{cases}
\end{aligned}
$$

Let $d^{c_1}_{s_a^i}(\alpha_i^*, \mathbf{s}^i)$ and $d^{c_1}_{\alpha_i}(\alpha_i^*, \mathbf{s}^i)$ be the subgradients of $C_{\alpha_i}(\tilde{\mathbf{c}}\mathbf{s}^i)$ with respect to s_a^i and α_i at point $(\alpha_i^*, \mathbf{s}^i)$, respectively. For our setting these gradients can be computed by:

$$
\begin{aligned}
d^{c_1}_{s_a^i}(\alpha_i^*, \mathbf{s}^i) &= \frac{\underline{c}_a(\overline{c}_a-\mu_a)\exp\left(\frac{(\underline{c}_a-\overline{c}_a)s_a^i}{\alpha_i}\right)+\overline{c}_a(\mu_a-\underline{c}_a)}{(\overline{c}_a-\mu_a)\exp\left(\frac{(\underline{c}_a-\overline{c}_a)s_a^i}{\alpha_i}\right)+\mu_a-\underline{c}_a} \\
d^{c_1}_{\alpha_i}(\alpha_i^*, \mathbf{s}^i) &= \sum_{a\in\mathcal{A}} \ln\left(\frac{(\overline{c}_a-\mu_a)\exp(\frac{\underline{c}_a s_a^i}{\alpha_i})+(\mu_a-\underline{c}_a)\exp(\frac{\overline{c}_a s_a^i}{\alpha_i})}{\overline{c}_a-\underline{c}_a}\right) + \\
&\quad \sum_{a\in\mathcal{A}}\left(\frac{s_a^i}{\alpha_i}\right)\left(\frac{\underline{c}_a(\overline{c}_a-\mu_a)\exp(\frac{\underline{c}_a s_a^i}{\alpha_i})+\overline{c}_a(\mu_a-\underline{c}_a)\exp(\frac{\overline{c}_a s_a^i}{\alpha_i})}{(\overline{c}_a-\mu_a)\exp(\frac{\underline{c}_a s_a^i}{\alpha_i})+(\mu_a-\underline{c}_a)\exp(\frac{\overline{c}_a s_a^i}{\alpha_i})}\right)
\end{aligned}
$$

Similar the subgradients of function $C_{\eta_i}(-\tilde{\mathbf{c}}\mathbf{s}^i)$ can be computed by:

$$
\begin{aligned}
d^{c_2}_{s_a^i}(\eta_i^*, \mathbf{s}^i) &= \frac{-\underline{c}_a(\overline{c}_a-\mu_a)\exp\left(\frac{(\overline{c}_a-\underline{c}_a)s_a^i}{\eta_i}\right)-\overline{c}_a(\mu_a-\underline{c}_a)}{(\overline{c}_a-\mu_a)\exp\left(\frac{(\overline{c}_a-\underline{c}_a)s_a^i}{\eta_i}\right)+\mu_a-\underline{c}_a} \\
d^{c_2}_{\alpha_i}(\eta_i^*, \mathbf{s}^i) &= \sum_{a\in\mathcal{A}} \ln\left(\frac{(\overline{c}_a-\mu_a)\exp(-\frac{\underline{c}_a s_a^i}{\eta_i})+(\mu_a-\underline{c}_a)\exp(-\frac{\overline{c}_a s_a^i}{\eta_i})}{\overline{c}_a-\underline{c}_a}\right) + \\
&\quad \sum_{a\in\mathcal{A}}\left(\frac{s_a^i}{\eta_i}\right)\left(\frac{-\underline{c}_a(\overline{c}_a-\mu_a)\exp(-\frac{\underline{c}_a s_a^i}{\eta_i})-\overline{c}_a(\mu_a-\underline{c}_a)\exp(-\frac{\overline{c}_a s_a^i}{\eta_i})}{(\overline{c}_a-\mu_a)\exp(-\frac{\underline{c}_a s_a^i}{\eta_i})+(\mu_a-\underline{c}_a)\exp(-\frac{\overline{c}_a s_a^i}{\eta_i})}\right)
\end{aligned}
$$

Appendix B: Proof convexity $f(\mathbf{s})$

Proposition 1 stating that $f(\mathbf{s})$ is convex in $\mathbf{s}$ is proven in this appendix.

L et $\boldsymbol{\alpha}^s, \boldsymbol{\eta}^s, \boldsymbol{\tau}^s$ and $\boldsymbol{\alpha}^y, \boldsymbol{\eta}^y, \boldsymbol{\tau}^y$ be the optimal solutions of $f(\mathbf{s})$ and $f(\mathbf{y})$. Since function $C_{\alpha_i}(\tilde{\mathbf{c}}\mathbf{s}^i)$ is jointly convex in $(\boldsymbol{\alpha_i}, \boldsymbol{s}^i)$, it implies that for any $i \in \mathcal{N}_T$ and $0 \leq \beta \leq 1$:

$$\begin{aligned} C_{\beta\alpha_i^s+(1-\beta)\alpha_i^y}(\tilde{\boldsymbol{c}}(\beta\mathbf{s}^i+(1-\beta)\mathbf{y}^i)) =& C_{\beta\alpha_i^s+(1-\beta)\alpha_i^y}(\beta\tilde{\mathbf{c}}\mathbf{s}^i+(1-\beta)\tilde{\boldsymbol{c}}\mathbf{y}^i) \\ \leq& \beta C_{\alpha_i^s}(\tilde{\mathbf{c}}\mathbf{s}^i)+(1-\beta)C_{\alpha_i^y}(\tilde{\mathbf{c}}\mathbf{y}^i) \\ \leq& \beta(\tau_i^s+\epsilon_i)+(1-\beta)(\tau_i^y+\epsilon_i) \\ =& \beta\tau_i^s+(1-\beta)\tau_i^y+\epsilon_i. \end{aligned}$$

Hence, there exists $(\boldsymbol{\alpha}', \boldsymbol{\eta}', \boldsymbol{\tau}')$, with $\boldsymbol{\alpha}' = \beta\boldsymbol{\alpha}^s + (1-\beta)\boldsymbol{\alpha}^y$, $\boldsymbol{\eta}' = \beta\boldsymbol{\eta}^s + (1-\beta)\boldsymbol{\eta}^y$ and $\boldsymbol{\tau}' = \beta\boldsymbol{\tau}^s + (1-\beta)\boldsymbol{\tau}^y$ such that

$$\begin{aligned} C_{\alpha_i'}(\tilde{\boldsymbol{c}}(\beta\mathbf{s}^i+(1-\beta)\mathbf{y}^i)) \leq \tau_i' + \epsilon_i \text{ for } \forall i \in \mathcal{N}_T \\ C_{\eta_i'}(-\tilde{\boldsymbol{c}}(\beta\mathbf{s}^i+(1-\beta)\mathbf{y}^i)) \leq -\tau_i' \text{ for } \forall i \in \mathcal{N}_T. \end{aligned}$$

Hence $\boldsymbol{\alpha}'$, $\boldsymbol{\eta}'$ and $\boldsymbol{\tau}'$ satisfy Constraints (22) and (23) and Constraints (24) and (25) are trivially satisfied. Therefore,

$$f(\beta\mathbf{s}+(1-\beta)\mathbf{y}) \leq \sum_{i\in\mathcal{N}_T} \beta(\alpha_i^s+\eta_i^s)+(1-\beta)(\alpha_i^y+\eta_i^y) = \beta f(\mathbf{s})+(1-\beta)f(\mathbf{y})$$

which indicates that $f(\mathbf{s})$ is convex in $\mathbf{s}$.

Appendix C: Arc selection measures

In this appendix, different arc selection methods are proposed to generate the arc set of the instances. Arcs with high mean travel time and a wide travel time distribution are unlikely to be used in the optimal solution. Let c_a be the mean travel time of arc a and let $\Delta_a = \overline{c}_a - \underline{c}_a$ be the difference between the maximum and minimum value of the travel time of arc a. To reduce the number of arcs, four different measures to rank the arcs are proposed and tested. Let $a = (i, j)$ be an arc, then the four measures are given by:

(i) c_a

(ii) Δ_a

(iii) $c_a \times \Delta_a$

(iv) $c_a / \mathbb{E}_{b\in\delta^-(j)} c_b + \Delta_a / \mathbb{E}_{b\in\delta^-(j)} \Delta_b$

In measure (iv) the mean travel time of arc (i, j) is divided by the average mean travel time of the incoming arcs of node j, to measure the performance of the arc relative to the other incoming arcs of node j. The same holds for the difference parameter Δ_a. Similarly, relative variants of measures (i)-(iii) can be generated.

Suppose there are N customers and we want to select approximately A arcs. 11 arc selection methods are tested: in arc selection methods 1-4, the arcs are selected based on increasing value of the measures (i)-(iv), in which at least $\lfloor A/2N \rfloor$ incoming arcs and $\lfloor A/2N \rfloor$ outgoing arcs have to be selected for every node. The same selection method is used in arc selection methods 5-7 but these are based on the relative variants of measures (i)-(iii), e.g., $c_a / \mathbb{E}_{b\in\delta^-(j)} c_b$ is measure 5. In arc selection method 8-11, the best $\lfloor A/N - 1 \rfloor$ incoming arcs and the best $\lfloor A/N - 1 \rfloor$ outgoing arcs based on measures (i)-(iv) are selected for every node. Note that

in measures 1–7 exactly A arcs are selected. However, in measures 8–11 there is overlap between arcs selected at every node so the number of arcs selected is not exactly equal to A.

The arc selection methods are tested on the triangular and gamma instances described in Section 7.1.1 with $A = 4N$ and $A = 5N$. Per arc selection method, the average results of the instances with $N = 10$ and $N = 20$ customers are presented in Table 10. In all arc selection methods, the arcs that are part of the VRP solution and the arcs from and to the depot that are not yet included in the arc set are added as well. The column "time" represent the average computational time in seconds and column "diff" reports the average increase in time window violation index compared to the best solution found by all measures, i.e., the denominator the best solution. The average results over all tests are summarized in the last two columns.

	10 customers				20 customers				Average	
	triangular		gamma		triangular		gamma			
Method	time	diff	time	diff	time	diff	time	diff	time	diff
1 - (i)	1.0	24%	4.2	11%	111.0	68%	2168.0	18%	571.1	30%
2 - (ii)	1.0	22%	1.4	12%	91.4	50%	224.0	24%	79.4	27%
3 - (iii)	**0.9**	18%	2.9	7%	104.5	52%	1572.8	15%	420.3	23%
4 - (iv)	1.1	18%	2.6	5%	142.4	45%	1260.6	7%	351.7	19%
5 - (i)	**0.9**	23%	5.8	8%	**76.5**	51%	1870.7	16%	488.5	24%
6 - (ii)	1.0	17%	**1.3**	13%	99.2	44%	**151.2**	26%	**63.2**	25%
7 - (iii)	1.1	18%	2.7	7%	134.0	44%	1441.3	9%	394.8	20%
8 - (i)	1.1	12%	6.5	7%	117.0	29%	2467.9	15%	648.1	16%
9 - (ii)	1.1	12%	2.5	9%	144.7	23%	276.5	23%	106.2	16%
10 - (iii)	1.0	**4%**	5.1	4%	122.5	**19%**	1976.3	5%	526.2	**8%**
11 - (iv)	1.0	**4%**	5.3	**3%**	137.8	**19%**	1982.3	**4%**	531.6	**8%**

Table 10 Computational time and solution quality of the different arc selection measures.

Arc selection methods 5-7, using the relative measures, perform slightly better than arc selection methods 1-3. Furthermore, arc selection methods 8-11, that select $\lfloor A/N - 1 \rfloor$ in and outgoing arcs per node, perform better than the other methods that select the arcs based on increasing value of the measures. Arc selection methods based on only the mean travel time (i) or on only the arc difference (ii) perform worse than methods using both parameters. The methods based on only the difference (ii) have a significantly lower computational time than the other methods while the methods based on only the mean travel time (i) have the highest computational time on average. Arc selection method 11 has the best trade-off between computational time and solution quality and this method shows the most robust performance over all instances. Therefore, arc selection method 11 will be used to generate the arc set of the instances.

In Table 11, the average results of arc selection measure 11 for different values of A are presented for the different instance sets. The column "risk" present the average time window violation index of the instance set. Table 11 shows that the computational time increases significantly when the number of customers increases from 10 to 20 and that the gamma based instances are more difficult to solve than the triangular instances. In many cases the time limit of two hours is reached when solving the 20 customer gamma instances with

$A = 6N$. When A increases, the computational time increases but the time window violation index decreases. On average, the difference in the violation index between $A = 4N$ and $A = 5N$ is small whereas the case $A = 6N$ is computationally much more demanding. Therefore, $A = 4N$ is used to generate the instances since this gives the best balance between computational time and solution quality.

	10 customers						20 customers					
	triangular			gamma			triangular			gamma		
A	risk	time	diff	risk	time	diff	risk	time	diff	risk	time	diff
$3N$	61.7	0.2	33%	126.1	0.5	12%	133.4	5.8	54%	399.9	58.2	19%
$4N$	54.8	0.6	5%	117.9	2.3	3%	106.6	44.2	23%	353.1	538.5	4%
$5N$	54.6	1.4	4%	116.7	8.3	2%	95.6	213.3	15%	347.0	2430.6	2%
$6N$	50.9	2.3	0%	116.1	18.0	1%	95.1	632.8	11%	344.8	4289.1	1%

Table 11 Average results of measure 11 for different numbers of arcs.

The characteristics of the new instances are given in the next Appendix D.

Appendix D: Characteristics of the instances

In Table 12 the characteristics of the instances are presented. The first column reports the number of customers in each instance. The average minimum, mean, and maximum values of the travel times of the arcs in the instances are presented in columns, "min", "μ", and "max", respectively. The average difference between the maximum and minimum value is given in column "Δ". The standard deviation of the mean arc length and the difference are presented in columns "sdμ" and "sdΔ", respectively. The average mean arc length decreases from G1 to G3 and from T1 to T3. Furthermore, the average difference between the maximum and minimum travel time, denoted by Δ, fluctuates with less than 1% between G1, G2, and G3 and between T1, T2, and T3.

	T1						T2						T3					
N	min	μ	max	Δ	sdμ	sdΔ	min	μ	max	Δ	sdμ	sdΔ	min	μ	max	Δ	sdμ	sdΔ
10	17.4	24.1	30.8	13.4	14.4	10.8	17.3	23.0	30.8	13.5	14.0	10.8	17.1	21.5	30.2	13.2	12.2	10.3
15	16.3	22.7	29.1	12.8	16.2	11.6	16.3	21.6	29.1	12.8	14.9	11.5	16.4	20.7	29.4	13.0	14.7	12.5
20	17.0	23.6	30.3	13.3	17.6	13.0	16.8	22.2	29.8	13.0	16.4	12.6	16.9	21.2	29.8	12.9	15.3	12.3
25	15.8	21.6	28.2	12.4	16.6	12.1	15.8	20.9	28.1	12.3	15.9	12.3	15.6	19.7	27.8	12.1	15.3	12.4
30	15.7	21.9	28.2	12.4	18.1	13.0	15.7	20.9	28.2	12.5	17.3	13.5	15.5	19.5	27.6	12.1	15.9	13.1
avg	16.5	22.8	29.3	12.8	16.6	12.1	16.4	21.7	29.2	12.8	15.7	12.1	16.3	20.5	29.0	12.7	14.7	12.1
	G1						G2						G3					
N	min	μ	max	Δ	sdμ	sdΔ	min	μ	max	Δ	sdμ	sdΔ	min	μ	max	Δ	sdμ	sdΔ
10	18.0	24.0	32.9	14.9	10.6	2.8	18.0	22.5	32.8	14.8	10.6	2.9	18.9	22.2	34.0	15.1	11.0	4.4
15	17.9	23.9	32.8	14.8	11.1	3.0	17.5	22.1	32.6	15.1	10.8	3.2	18.0	21.2	32.7	14.7	11.0	4.2
20	18.4	24.3	33.0	14.6	11.7	2.9	18.2	22.6	32.7	14.5	11.9	3.0	18.9	22.0	33.3	14.4	12.0	4.1
25	17.4	23.2	31.9	14.5	11.7	2.9	17.3	21.8	31.9	14.6	11.4	3.0	17.8	20.9	32.2	14.5	11.4	4.3
30	17.5	23.2	31.9	14.4	12.3	2.9	17.4	21.7	31.8	14.5	12.1	3.0	17.7	20.8	32.1	14.4	12.2	4.2
avg	17.9	23.7	32.5	14.6	11.5	2.9	17.7	22.1	32.4	14.7	11.4	3.0	18.2	21.4	32.9	14.6	11.5	4.3

Table 12 Characteristics of the instances.

Appendix E: Detailed results branch-and-cut algorithm

The detailed results of the triangular and gamma instances are presented in Tables 13 and 14, respectively. The instance number is denoted in the first column and the number of customers N in the second column. The number of vehicle used in the final solution is reported in the column "nV" and the computational time in seconds is reported in the column "time". The upper bound of the time window violation index is presented in column "risk" and the lower bound in presented in column 'LB'. The number of subgradient cuts added to the formulation is presented in the column "nC". In columns "Δrisk" and "Δtt", the relative difference of the violation index and the travel time compared to the VRP-based solution are given. The difference is computed by $(R-R_0)/R_0$, with R_0 denoting the violation index corresponding to the VRP-based solution and R the violation index of the RVRP-TWA solution. A similar calculation is performed for the difference in travel time. If an instance is not solved within two hours and the upper bound of time window violation index is equal to zero, then no feasible solution is found and this solution is not taken into account when calculating the average values.

Appendix F: Fixed $\boldsymbol{\tau}$ policy

In this appendix, we present the adjustment of the solution method when the value of τ_i is not a decision variable but a fixed value equal to $\tau_i = \mathbf{cs}^i - \epsilon_i/2$, $\tau_i = \mathbf{cs}^i - \epsilon_i$ or $\tau_i = \mathbf{cs}^i$. We will show this adjustment for the first case in which the time windows are symmetrically around the average arrival time. In this case, the minimum time window violation index of routing solution $\mathbf{s}$ is given by

$$\begin{aligned} f(\mathbf{s}) = \inf \ & \sum_{i\in\mathcal{N}_T} \alpha_i + \eta_i & \\ s.t.\ & C_{\alpha_i}(\tilde{\mathbf{cs}}^{\mathrm{i}}) \le \mathbf{cs}^i + \frac{\epsilon_i}{2}, & \forall i \in \mathcal{N}_T, \\ & C_{\eta_i}(-\tilde{\mathbf{cs}}^{\mathrm{i}}) \le -\mathbf{cs}^i + \frac{\epsilon_i}{2}, & \forall i \in \mathcal{N}_T, \\ & \alpha_i, \eta_i \ge 0, & \forall i \in \mathcal{N}_T. \end{aligned}$$

The Lagrange function is equal to

$$L(\mathbf{s},\boldsymbol{\alpha},\boldsymbol{\eta},\boldsymbol{\lambda}) = \sum_{i\in\mathcal{N}_T} \alpha_i + \sum_{i\in\mathcal{N}_T} \eta_i + \sum_{i\in\mathcal{N}_T} \overline{\lambda}(C_{\alpha_i}(\tilde{\mathbf{cs}}^i) - \mathbf{cs}^i - \frac{\epsilon_i}{2}) + \sum_{i\in\mathcal{N}_T} \underline{\lambda}(C_{\eta_i}(-\tilde{\mathbf{cs}}^i) + \mathbf{cs}^i + \frac{\epsilon_i}{2}).$$

With the same reasoning as in Section 4, the subgradient of $f(\mathbf{s})$ is equal to the derivative of the Lagrange function with respect to $\mathbf{s}$. This is equal to

$$d^L_{s^i_a}(\mathbf{s},\boldsymbol{\alpha^*},\boldsymbol{\eta^*},\boldsymbol{\lambda^*}) = \overline{\lambda}^* d^{c_1}_{s^i_a}(\alpha^*_i,\mathbf{s}^i) + \underline{\lambda}^* d^{c_2}_{s^i_a}(\eta^*_i,\mathbf{s}^i) + \tilde{c}_a(\underline{\lambda}^* - \overline{\lambda}^*). \tag{60}$$

With $\overline{\lambda}^* = \frac{-1}{d^{c_1}_{\alpha_i}(\alpha^*_i,s^i)}$ and $\underline{\lambda}^* = \frac{-1}{d^{c_2}_{\eta_i}(\eta^*_i,s^i)}$. For both $\tau_i = \mathbf{cs}^i - \epsilon_i$ and $\tau_i = \mathbf{cs}^i$ the derivative of $f(\mathbf{s})$ is also equal to equation (60).

		T1							T2							T3						
Inst	N	nV	time	risk	LB	nC	Δrisk	Δtt	nV	time	risk	LB	nC	Δrisk	Δtt	nV	time	risk	LB	nC	Δrisk	Δtt
c1	10	1	0	0	0	2	0%	1%	1	0	0	0	7	0%	5%	1	0	0	0	2	0%	3%
c2	10	1	1	15	15	6	-45%	4%	1	0	24	24	7	-34%	3%	1	0	97	97	8	-3%	3%
r1	10	1	0	102	102	10	-7%	3%	1	0	86	86	7	-27%	4%	1	0	129	129	4	0%	0%
r2	10	1	0	60	60	7	-50%	4%	1	1	177	177	9	0%	0%	1	0	138	138	3	-36%	4%
rc1	10	2	0	10	10	4	-69%	5%	2	2	1	1	29	-99%	3%	2	2	66	66	19	-47%	4%
rc2	10	1	0	27	27	6	0%	0%	1	1	43	43	16	-65%	4%	1	0	13	13	5	-62%	5%
avg		1.2	0	36	36	6	-13%	3%	1.2	1	55	55	13	-38%	3%	1.2	1	74	74	7	-25%	3%
c1	15	2	2	0	0	2	-100%	2%	2	16	3	3	12	-70%	3%	2	8	0	0	14	-100%	4%
c2	15	1	4	51	51	12	-10%	4%	1	3	80	80	10	-3%	5%	1	2	127	127	7	-4%	4%
r1	15	2	23	42	42	16	-78%	5%	2	41	52	52	27	-58%	3%	2	10	45	45	16	-38%	5%
r2	15	1	9	108	108	23	-63%	5%	1	3	117	117	8	-52%	5%	1	5	194	194	11	-16%	4%
rc1	15	2	5	1	1	20	-69%	2%	2	31	11	11	45	-39%	4%	2	9	5	5	10	-93%	4%
rc2	15	1	6	17	17	17	-25%	1%	1	6	48	48	19	-15%	1%	1	5	38	38	23	-16%	4%
avg		1.5	8	37	37	15	-57%	3%	1.5	17	52	52	20	-40%	3%	1.5	6	68	68	14	-44%	4%
c1	20	2	15	4	4	5	0%	2%	2	92	5	5	21	-59%	4%	2	31	0	0	7	-6%	4%
c2	20	1	4	108	108	7	0%	0%	1	12	87	87	10	-46%	5%	1	12	114	114	20	-20%	4%
r1	20	2	21	133	133	7	-31%	3%	2	87	103	103	32	-71%	4%	2	31	136	136	17	-2%	3%
r2	20	1	13	288	288	12	-23%	5%	1	55	211	211	41	-24%	3%	1	10	335	335	10	-34%	4%
rc1	20	3	60	33	33	32	-34%	5%	3	214	3	3	63	-69%	2%	3	99	34	34	41	-84%	4%
rc2	20	1	20	59	59	41	-40%	2%	1	13	81	81	24	-11%	1%	1	6	186	186	9	-58%	4%
avg		1.7	22	104	104	17	-21%	3%	1.7	79	81	81	32	-47%	3%	1.7	31	134	134	17	-34%	4%
c1	25	3	29	0	0	11	-98%	5%	3	33	0	0	18	-100%	5%	3	37	0	0	10	0%	3%
c2	25	2	834	36	36	40	-37%	5%	2	1674	33	33	67	-63%	5%	2	754	43	43	42	-34%	5%
r1	25	3	2740	124	124	25	-37%	4%	2	347	433	433	12	-3%	1%	2	827	105	105	45	-18%	5%
r2	25	2	1788	139	139	66	-74%	5%	1	106	501	501	12	0%	0%	1	723	258	258	138	-39%	3%
rc1	25	3	577	3	3	102	-62%	3%	3	169	3	3	60	-48%	4%	3	288	5	5	56	-84%	5%
rc2	25	1	37	135	135	34	-6%	4%	1	102	86	86	45	-26%	5%	1	314	107	107	167	-13%	4%
avg		2.3	1001	73	73	46	-52%	4%	2.0	405	176	176	36	-40%	3%	2.0	491	86	86	76	-31%	4%
c1	30	3	462	0	0	25	-98%	5%	3	450	5	5	72	-58%	5%	3	467	1	1	34	-89%	5%
c2	30	2	7200	118	0	28	-40%	5%	2	7200	53	0	89	-26%	4%	2	7200	28	0	57	-71%	2%
r1	30	3	7200	80	0	31	-38%	4%	3	5091	110	110	62	-34%	5%	3	6157	69	69	69	-42%	5%
r2	30	2	7200	132	0	31	-58%	5%	2	3784	218	218	52	-54%	4%	2	7200	324	0	13	-26%	4%
rc1	30	4	7200	6	2	69	-49%	5%	4	7200	28	25	140	-31%	5%	4	7200	73	64	58	-68%	5%
rc2	30	1	265	308	308	6	-12%	0%	1	234	372	372	49	-2%	2%	1	2421	612	612	240	-1%	1%
avg		2.5	4921	107	52	32	-49%	4%	2.5	3993	131	122	77	-34%	4%	2.5	5108	185	125	79	-49%	4%
c1	35	4	7200	7	0	53	-54%	5%	4	3650	1	1	44	-96%	4%	4	7200	3	0	46	-53%	5%
c2	35	2	7200	0	0	0	-100%	0%	2	7200	86	0	28	0%	4%	2	7200	88	0	39	0%	2%
r1	35	3	7200	135	0	35	-29%	5%	3	7200	220	0	5	-9%	4%	3	7200	117	0	37	-24%	4%
r2	35	2	7200	232	0	109	-21%	4%	2	7200	276	0	19	-41%	5%	2	7200	176	0	76	-25%	4%
rc1	35	4	7200	12	4	96	-73%	5%	4	7200	79	38	90	-22%	4%	4	7200	16	0	128	-93%	5%
rc2	35	2	7200	257	0	25	0%	5%	2	7200	131	25	80	-3%	1%	2	1028	192	192	84	-36%	5%
avg		2.8	7200	128	1	64	-35%	5%	2.8	6608	132	11	44	-28%	4%	2.8	6171	99	32	68	-38%	4%

Table 13 Detailed results of the triangular instances.

Appendix G: Description of the MT distribution

In this appendix, alternative distributions are generated for the original triangular and gamma instances described in Section 7.1. The original travel time distribution of arc a is characterized by a minimum value $\underline{c}_a$, maximum value $\overline{c}_a$, and mean value c_a. The mode of the distributions is denoted by m_a. The new generated alternative distribution is a mixture of two triangular distributions which both have probability 1/2. This new distribution will be denoted by MT and the two triangular distributions of which the MT distribution

		G1							G2							G3						
Inst	N	nV	time	risk	LB	nC	Δrisk	Δtt	nV	time	risk	LB	nC	Δrisk	Δtt	nV	time	risk	LB	nC	Δrisk	Δtt
c1	10	1	2	152	152	32	-22%	4%	1	3	104	104	44	-25%	4%	1	2	76	76	25	-26%	4%
c2	10	1	2	156	156	28	-22%	5%	1	1	119	119	7	-20%	4%	1	1	86	86	9	-50%	3%
r1	10	1	0	176	176	6	-14%	5%	1	0	201	201	3	-6%	4%	1	0	159	159	2	0%	0%
r2	10	1	0	127	127	7	-5%	5%	1	0	152	152	5	-7%	3%	1	0	145	145	3	-3%	4%
rc1	10	2	9	73	73	69	-30%	2%	2	7	64	64	52	-31%	5%	2	6	38	38	45	-45%	4%
rc2	10	1	4	116	116	78	-22%	5%	1	4	113	113	57	-28%	5%	1	2	67	67	18	-33%	4%
avg		1.2	3	133	133	37	-19%	4%	1.2	2	125	125	28	-19%	4%	1.2	2	95	95	17	-26%	3%
c1	15	2	49	111	111	61	-22%	3%	2	136	114	114	175	-28%	3%	2	30	54	54	31	-29%	5%
c2	15	1	11	377	377	25	-13%	5%	1	10	321	321	23	-28%	2%	1	3	244	244	6	-15%	3%
r1	15	2	13	119	119	20	-38%	4%	2	15	152	152	16	-19%	5%	2	9	124	124	6	-40%	4%
r2	15	1	22	338	338	36	-31%	4%	1	5	320	320	18	-21%	4%	1	2	306	306	4	-1%	3%
rc1	15	2	291	113	113	262	-30%	4%	2	30	98	98	84	-20%	5%	2	93	71	71	102	-51%	4%
rc2	15	1	3	339	339	22	-9%	5%	1	12	329	329	67	-25%	5%	1	9	256	256	25	-31%	5%
avg		1.5	65	233	233	71	-24%	4%	1.5	35	222	222	64	-23%	4%	1.5	24	176	176	29	-28%	4%
c1	20	3	5777	244	244	162	-19%	4%	3	4957	195	195	197	-23%	4%	2	119	261	261	7	-9%	4%
c2	20	2	235	276	276	15	-51%	4%	2	126	323	323	29	-42%	5%	2	103	227	227	8	-61%	4%
r1	20	2	30	283	283	11	-17%	3%	2	43	243	243	15	-17%	4%	2	78	208	208	18	-25%	5%
r2	20	1	43	593	593	36	-12%	4%	1	24	622	622	25	-13%	5%	1	41	562	562	22	-23%	5%
rc1	20	3	5534	185	185	635	-29%	4%	3	792	172	172	276	-17%	5%	3	806	112	112	155	-33%	4%
rc2	20	1	202	596	596	112	-26%	3%	1	64	556	556	95	-12%	5%	1	33	364	364	32	-33%	5%
avg		2.0	1970	363	363	162	-26%	4%	2.0	1001	352	352	106	-21%	5%	1.8	197	289	289	40	-31%	5%
c1	25	3	4771	267	267	152	-17%	4%	3	5124	214	214	206	-19%	4%	3	2999	137	137	183	-31%	5%
c2	25	2	7200	427	0	130	-14%	5%	2	1499	472	472	44	-28%	4%	2	5474	329	329	96	-56%	4%
r1	25	3	7200	267	3	59	-18%	5%	3	4582	246	246	73	-57%	4%	2	91	443	443	2	0%	0%
r2	25	2	826	499	499	39	-23%	5%	2	3444	426	426	77	-52%	5%	1	38	991	991	4	0%	2%
rc1	25	3	7200	232	0	380	-30%	4%	3	7200	232	0	302	-19%	4%	3	5769	162	162	291	-34%	4%
rc2	25	1	770	1008	1008	196	-18%	4%	1	7200	771	92	431	-27%	3%	1	979	615	615	198	-36%	5%
avg		2.3	4661	450	296	159	-20%	4%	2.3	4842	394	242	189	-34%	4%	2.0	2558	446	446	129	-26%	3%
c1	30	4	7200	0	0	0.0	-100%	0%	3	7200	1542	98	82	-6%	4%	3	7200	277	55	36	-18%	5%
c2	30	2	7200	0	0	0	-100%	0%	2	7200	715	0	17	-31%	5%	2	7200	530	0	12	-13%	5%
r1	30	3	7200	510	0	13	-11%	3%	3	4995	440	440	70	-17%	5%	3	1478	293	293	53	-13%	4%
r2	30	2	7200	699	0	29	-47%	4%	2	7200	674	0	43	-27%	5%	2	7200	559	0	33	-56%	4%
rc1	30	4	7200	289	0	69	-17%	4%	4	7200	243	0	157	-19%	5%	4	7200	161	5	108	-27%	5%
rc2	30	2	7200	658	97	323	-30%	5%	2	7200	650	55	245	-20%	5%	2	7200	415	0	260	-30%	5%
avg		2.8	7200	539	24	109	-26%	4%	2.7	6833	711	99	102	-20%	5%	2.7	6246	373	59	84	-26%	5%

Table 14 Detailed results of the gamma instances.

exists are described as follows. The first triangular distribution has minimum value $\underline{c}_a$, maximum value equal to m and mode equal to $\frac{\underline{c}_a+m}{2}$. Therefore, the mean value of this distribution is equal to $\frac{\underline{c}_a+m}{2}$. Since the characteristics of the MT distribution should be equal to the characteristics of the original distribution, the mean value of the second distribution should be equal to $2c_a - \frac{\underline{c}_a+m}{2}$. The maximum value of the second distribution should be equal to $\overline{c}_a$ and the minimum value of the second distribution is chosen as high as possible. Two examples of the new distribution of a triangular and gamma distribution are presented in Figure 4.

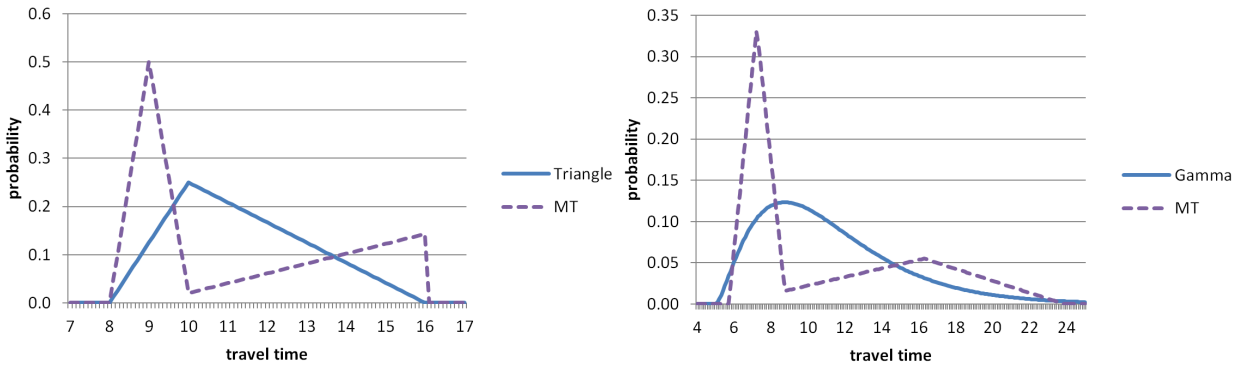

Figure 4 The original and new distribution of a triangular (left) and gamma distribution (right).

References

Adulyasak Y, Jaillet P, 2016 *Models and algorithms for stochastic and robust vehicle routing with deadlines. Transportation Science* 50(2):608–626.

Agatz N, Campbell A, Fleischmann M, Savelsbergh M, 2011 *Time slot management in attended home delivery. Transportation Science* 45(3):435–449.

Agra A, Christiansen M, Figueiredo R, Hvattum LM, Poss M, Requejo C, 2013 *The robust vehicle routing problem with time windows. Computers & Operations Research* 40(3):856–866.

Bertsimas D, Sim M, 2004 *The price of robustness. Operations Research* 52(1):35–53.

Campbell AM, Savelsbergh M, 2006 *Incentive schemes for attended home delivery services. Transportation Science* 40(3):327–341.

Dalmeijer K, Spliet R, 2018 *A branch-and-cut algorithm for the time window assignment vehicle routing problem. Computers & Operations Research* 89:140–152.

Ehmke JF, Campbell AM, Urban TL, 2015 *Ensuring service levels in routing problems with time windows and stochastic travel times. European Journal of Operational Research* 240(2):539–550.

Ellis B, 2011 *Waiting for the cable guy is costing us $38 billion.* URL `http://money.cnn.com/2011/11/03/pf/costofwaiting/index.htm`.

Gendreau M, Jabali O, Rei W, 2016 *50th anniversary invited article—future research directions in stochastic vehicle routing. Transportation Science* 50(4):1163–1173.

Golden BL, Raghavan S, Wasil EA, 2008 *The vehicle routing problem: latest advances and new challenges*, volume 43 (Springer).

Jabali O, Leus R, Van Woensel T, De Kok T, 2015 *Self-imposed time windows in vehicle routing problems. OR Spectrum* 37(2):331–352.

Jaillet P, Qi J, Sim M, 2016 *Routing optimization under uncertainty. Operations Research* 64(1):186–200.

Klein R, Neugebauer M, Ratkovitch D, Steinhardt C, 2017 *Differentiated time slot pricing under routing considerations in attended home delivery. Transportation Science* 53(1):236–255.

Laporte G, Louveaux F, Mercure H, 1992 *The vehicle routing problem with stochastic travel times. Transportation Science* 26(3):161–170.

Lee C, Lee K, Park S, 2012 *Robust vehicle routing problem with deadlines and travel time/demand uncertainty. Journal of the Operational Research Society* 63(9):1294–1306.

Lysgaard J, Letchford AN, Eglese RW, 2004 *A new branch-and-cut algorithm for the capacitated vehicle routing problem. Mathematical Programming* 100(2):423–445.

Ordóñez F, 2010 *Robust vehicle routing. In INFORMS TutORials in Operations Research.*, 153–178 (Published online: 14 Oct 2014).

Russell R, Urban T, 2008 *Vehicle routing with soft time windows and erlang travel times. Journal of the Operational Research Society* 59(9):1220–1228.

Solomon MM, 1987 *Algorithms for the vehicle routing and scheduling problems with time window constraints. Operations Research* 35(2):254–265.

Spliet R, Dabia S, Van Woensel T, 2017 *The time window assignment vehicle routing problem with time-dependent travel times. Transportation Science* 52(2):261–276.

Spliet R, Gabor AF, 2014 *The time window assignment vehicle routing problem. Transportation Science* 49(4):721–731.

Subramanyam A, Gounaris CE, 2017 *Strategic allocation of time windows in vehicle routing problems under uncertainty. Proceedings of the Foundations of Computer-Aided Process Operations/Chemical Process Control (FOCAPO 2017/CPC IX)* 62.

Taş D, Dellaert N, Van Woensel T, De Kok T, 2013 *Vehicle routing problem with stochastic travel times including soft time windows and service costs. Computers & Operations Research* 40(1):214–224.

Taş D, Dellaert N, van Woensel T, de Kok T, 2014 *The time-dependent vehicle routing problem with soft time windows and stochastic travel times. Transportation Research Part C: Emerging Technologies* 48:66–83.

Toth P, Vigo D, 2014 *Vehicle routing: problems, methods, and applications, Second Edition* (Society for Industrial & Applied Mathematics (SIAM), Philadelphia).

Ulmer MW, Thomas BW, 2019 *Enough waiting for the cable guy—estimating arrival times for service vehicle routing. Transportation Science* Articles in Advance, 7 Feb 2019.

Vareias AD, Repoussis PP, Tarantilis CD, 2017 *Assessing customer service reliability in route planning with self-imposed time windows and stochastic travel times. Transportation Science* 53(1):256–281.

Zhang C, Nemhauser G, Sokol J, Cheon M, Papageorgiou D, 2015 *Robust inventory routing with flexible time window allocation. Working paper. Available on Optimization Online* .

Zhang Y, Baldacci R, Sim M, Tang J, 2019 *Routing optimization with time windows under uncertainty. Mathematical Programming* 175(1-2):263–305.

Zhang Y, Zhang Z, Lim A, Sim M, 2018 *Robust data-driven vehicle routing with time windows. Working paper. Available on Optimization Online* .